Alina Humnig, BSc

The role of spermidine in the regulation of IGF-1/PI3K signaling pathway in the mouse heart

MASTER'S THESIS

to achieve the university degree of

Master of Science

Master's degree programme: Biochemistry and Molecular Biomedical Sciences

submitted to

Graz University of Technology

Supervisor

Assoz. Prof. Dr.rer.nat. Simon Sedej

Medical University of Graz, Department of Cardiology

Graz, March 2018

Affidavit

I declare that I have authored this thesis independently, that I have not used other than the declared sources/resources, and that I have explicitly indicated all material which has been quoted either literally or by content from the sources used. The text document uploaded to TUGRAZonline is identical to the present master's thesis.

Graz, March 2018 ....

Acknowledgement

I would first like to express my sincere gratitude to my supervisor Simon Sedej for his patient guidance, encouragement and advice he provided throughout my time in this lab. His door was always open whenever I had a question about my research or writing. Without his constant support, critical advices, and continuous supervision this thesis would not have been possible. I could not have imagined a better supervisor for my master thesis.

Besides my supervisor, special thanks goes to Viktoria Herbst, who patiently inducted me into all the working procedures and giving me a helping hand whenever I needed one. You are really the good soul of this working group who keeps the lab running.

I also want to thank Mahmoud Abdellatif for his support and helping me with my statistics. You are really the most ambitious and inquisitive person I have ever met. Keep that up!

Special thanks go to my friends, who motivated and supported me throughout my time as a student. Especially I want to thank my two Sarahs, who always had a friendly ear and always helping me through the hard times. Thank you for this special time with you and being the best friends, I can imagine.

I want to particularly thank my boyfriend Aron. Although, it was not always easy with me, he supported me no matter what. Thank you for your unconditional patience, understanding and emotional support.

Last but not least, I want to express special thanks to my family for supporting me throughout all the years of my studies. I cannot tell how grateful I am for your encouragement. Thank you for always standing by my side and believing in me throughout all my life.

Table of Contents

Abstract

Over the last decades the lifespan has substantially increased and the rise in life expectancy in most developed countries is projected further to grow in the 21st century. Despite intensive research efforts to combat age-related cardiovascular disease, the leading cause of death worldwide, there are no effective agents to slow cardiac aging, mostly because the mechanisms and signaling pathways driving cardiac aging have been understudied. One such longevity pathway regulating aging-associated cardiac changes is the insulin-like growth factor-1/phosphoinositide 3-kinase (IGF-1/PI3K) signaling pathway.

Recently the potent autophagy inducer and natural polyamine spermidine was shown to inhibit IGF-1/PI3K/Akt signaling in skeletal muscle. The aim of this study was to elucidate whether cardioprotective effects by spermidine are mediated, at least in part, through the IGF-1/PI3K/Akt signaling pathway. We tested the hypothesis that spermidine inhibits the IGF-1/PI3K/Akt signaling pathway in the mouse heart. To this end, we performed immunoblot analysis of heart lysates from middle-aged (12-month-old) male mice overexpressing cardiomyocyte-specific IGF-1 receptor (IGF-1R) upon oral spermidine treatment (for 5 months in drinking water). In addition, we used mice harbouring cardiomyocyte-specific inhibition of PI3K (dnPI3K) that were subjected to single (acute) intraperitoneal application of spermidine. Our results show that IGF-1R mice had markedly increased expression of IGF-1R, which was significantly reduced upon chronic supplementation of spermidine. In contrast, spermidine treatment did not change the expression of IGF-1R in WT animals. Although the expression of IGF-1/PI3K downstream target Akt was significantly reduced in mice overexpressing IGF-1R under control conditions, phosphorylation at Thr308 and Ser473 sites was clearly elevated, implying increased activation of the IGF-1/PI3K signaling in IGF-1 hearts. Chronic spermidine administration did not significantly change the expression and phosphorylation of Akt as well as mTOR expression in WT and IGF-1R mice. However, we found that acute application of spermidine reduced the phosphorylation of Akt at Thr308 site and phosphorylation of the Forkhead box transcription factor 3a (FoxO3a) at Ser253 site in WT hearts, while these effects were not observed in dnPI3K mice. Our results suggest that spermidine inhibits, at least in part, the IGF-1/PI3K/Akt signaling pathway in the heart. Phosphorylation of Akt at Thr308 site and dephosphorylation of FoxO3a seem to be important downstream targets of the IGF-1/PI3K signaling pathway underlying cardioprotective effects by spermidine. Further investigation is warranted to elucidate the precise role of spermidine in this complex molecular pathway driving cardiac aging.

Zusammenfassung

In den letzten Jahrzehnten ist die Lebenserwartung in der Bevölkerung deutlich angestiegen und wird laut Prognosen auch im 21. Jahrhundert weiterhin zunehmen. Herz-Kreislauf-Erkrankungen zählen zu den weltweit häufigsten Todesursachen in der älteren Bevölkerung. Trotz intensiver Forschungsarbeit in der Bekämpfung von Herz-Kreislauf-Erkrankungen, gibt es derzeit noch keine wirksamen Therapien, um der Herzalterung entgegenzuwirken. Mechanismen und Prozesse, die mit der Alterung des Herzens assoziiert werden, sind weitgehendst noch nicht genügend erforscht. Ein wichtiger Signalweg im Kontext mit der Lebensdauer ist der insulinähnliche Wachstumsfaktor-1/Phosphoinositid-3-Kinase (IGF-1/PI3K) -Signalweg, welcher bekannt dafür ist, altersassoziierte Veränderungen im Herzen zu regulieren. Es konnte kürzlich gezeigt werden, dass das natürliche Polyamin Spermidin, ein potenter Autophagie-Induktor, den IGF-1/PI3K/Akt-Signalweg in der Skelettmuskulatur von Mäusen hemmt. Das Ziel dieser Studie war es zu klären, ob kardioprotektive Effekte durch Spermidin zumindest teilweise über den IGF-1/PI3K/Akt-Signalweg vermittelt werden.

Es wurde die Hypothese getestet, dass Spermidin den IGF-1/PI3K/Akt-Signalweg auch im Herzen hemmt. Zu diesem Zweck wurde Immunoblot-Analysen mit Herzlysaten von 12 Monate alten männlichen Mäusen, die eine kardiomyozyten-spezifische Überexpression des IGF-1 Rezeptors (IGF-1R) aufweisen, durchgeführt. Die Mäuse erhielten für 5 Monate Spermidin supplementiert im Trinkwasser. Zusätzlich wurden in diesen Experimenten Mäuse verwendet, die eine kardiomyozyten-spezifische Hemmung von PI3K (dnPI3K) aufweisen. Diese Mäuse wurden einer einzelnen (akuten) intraperitonealen Verabreichung von Spermidin unterzogen.

Unsere Ergebnisse zeigen, dass IGF-1R-Mäuse eine deutlich erhöhte Expression von IGF-1R zeigen, die bei chronischer Supplementation von Spermidin signifikant reduziert wird. Im Gegensatz dazu veränderte die Behandlung mit Spermidin die Expression von IGF-1R in Wildtypen nicht. Obwohl die Expression von Akt in Mäusen, die den IGF-1R überexprimieren, signifikant reduziert war, war die Phosphorylierung an den Phosphorylierungsstellen Thr308 und Ser473 stark erhöht, was eine erhöhte Aktivierung des IGF-1/PI3K-Signalwegs in IGF-1-Herzen unter Kontrollbedingungen impliziert Des Weiteren konnten wir zeigen, dass die chronische Behandlung mit Spermidin die Expression und Phosphorylierung von Akt, sowie die Expression von mTOR in WT- und IGF-1R- Mäusen nicht signifikant verändert. Jedoch konnte gezeigt werden, dass die akute Applikation von Spermidin die Phosphorylierung von Akt an der Stelle Thr308 und die Phosphorylierung des Forkhead-Box-Transkriptionsfaktors 3a (FoxO3a) an der Stelle Ser253 in WT-Herzen reduzierte. Diese Effekte wurden bei dnPI3K-

7

Mäusen nicht beobachtet. Unsere Ergebnisse weisen darauf hin, dass orale Supplementierung von Spermidin oder intraperitoneale Injektionen von Spermidin zumindest teilweise den IGF-1/PI3K/Akt-Signalweg im Herzen hemmen. Die Phosphorylierung von Akt an der Stelle Thr308 und die Dephosphorylierung von FoxO3a scheinen wichtige Ziele downstream im IGF-1/PI3K Signalwegs darzustellen. Diese scheinen den kardioprotektiven Effekte von Spermidin zugrunde zu liegen.

Weitere Untersuchungen sind erforderlich, um die genaue Rolle von Spermidin in diesem komplexen molekularen Signalweg, der mit der Alterung des Herzens assoziiert wird, aufzuklären.

1   Introduction

Over the last decades the lifespan has substantially increased and the rise in life expectancy in most developed countries is projected further to grow in the 21st century [1]. Despite the fact that statistical data show reduced mortality of the population > 80 years of age [2], the number of old people with poor health and chronic disability has been expanding [3]. Therefore, the healthcare and socioeconomic systems are challenged to reduce the disease burden in the elderly population [4]. Aging is by far the major independent risk factor for the development of cardiovascular disease (CVD) [5], the leading cause of death worldwide in the elderly [6]. Despite intensive research efforts to combat CVD, there is an urgent need to improve current understanding of mechanisms and processes underlying aging-associated cardiac changes in order to develop effective, preventive and therapeutic treatments against cardiac aging.

One such mechanism involved in cardiac aging and longevity, is the insulin-like growth factor 1 (IGF-1) signaling pathway. Studies conducted in several model organisms showed disparate impact of IGF-1 pathway on cardiovascular effect and longevity [7, 8]. Considering such controversial findings from animal and human studies it seems clear that the role of this evolutionary conserved pathway on cardiac aging is far from resolved. So far, regulation of the activity of the IGF-1/PI3K signaling pathway is perhaps the most validated and consistent intervention to delay cardiac aging or the onset of cardiovascular disease in the elderly and so to extend the lifespan [9, 10].

The aim of this study was to examine the role of the IGF-1 signaling pathway and its downstream targets in the mouse heart. Furthermore, we investigated whether cardioprotective effects by spermidine are mediated, at least partially, through the IGF-1/PI3K/Akt signaling pathway. To this end, we tested the hypothesis that spermidine supplementation (acute or chronic) inhibits the IGF-1/PI3K/Akt signaling pathway in the mouse heart.

1.1   Structural and functional changes of the heart in aging

The majority of cardiomyocytes in the adult heart are terminally-differentiated cells, and thus have only limited ability to proliferate. Less than half of all cardiomyocytes are exchanged (i.e. renewed) during a normal lifespan [11], which leads to the accumulation of damaged cellular material (e.g. long-lived and/or misfolded proteins, dysfunctional and damaged mitochondria) and alters functional and structural homeostasis of the aging heart due to impaired repair mechanisms. Such age-associated alterations may cause apoptosis and/or necrosis, leading to

changes in the cellular composition of the heart due to decreased number of cardiomyocytes [12, 13]. Depleted pool of viable cardiomyocytes cannot be sufficiently replaced, because the cardiac stem cells capacity of regeneration declines with advanced age [14, 15]. This age-associated loss of functional cardiomyocytes promotes several structural and functional changes, including left ventricular hypertrophy (LVH) and fibrosis (Figure 1). Cardiac hypertrophy, a typical hallmark of cardiac aging [16], is characterized by an increase in size of cardiomyocytes and, therefore, increased left ventricular wall thickness. Hypertrophic growth is an adaptive mechanism to normalize left ventricular wall stress and elevated oxygen demand. Such left ventricular remodeling is necessary to maintain the cardiac output in order to meet the body´s demands (e.g. during exercise) [17, 18]. In addition to hypertrophy, increased cardiac fibrosis and arterial stiffness due to increased accumulation and intermolecular cross-linking of collagen in the myocardium and vasculature, respectively, are common age-associated structural changes. Increased synthesis or decreased degradation of the fibrotic extracellular matrix (ECM), generated by cardiac fibroblasts, is associated with increased passive stiffness of the heart and vessels as well as age-related diastolic dysfunction due to impaired relaxation and reduced filling of the left ventricle [19, 20]. Another mechanism that contributes to the age-dependent diastolic dysfunction is reduced active relaxation of cardiomyocytes, which occurs due to the disturbances in intracellular Ca^{2+} cycling, reduced Ca^{2+} sensitivity of the myofilament proteins and alterations in actin or myosin properties [21].

A large body of evidence has shown that mitochondrial function declines with age in virtually all organs, including the heart [6]. Cardiomyocytes are metabolically highly active and energy demanding cells with a high number of mitochondria, and therefore it is not surprising, that age-related alterations of mitochondria have been related to cardiac aging. Factors that contribute to mitochondrial dysfunction and reduced energetic capacity of the cardiac mitochondria include loss of cristae, deficient ATP production, increased production of reactive oxygen species (ROS), increased number of mitochondrial DNA (mtDNA) mutations, reduced mitophagy (i.e. mitochondrial autophagy) and respiratory chain malfunction [22]. Numerous studies have shown that mitochondrial metabolism is important in mediating longevity through nutrient-sensing pathways and dietary restriction [23–25].
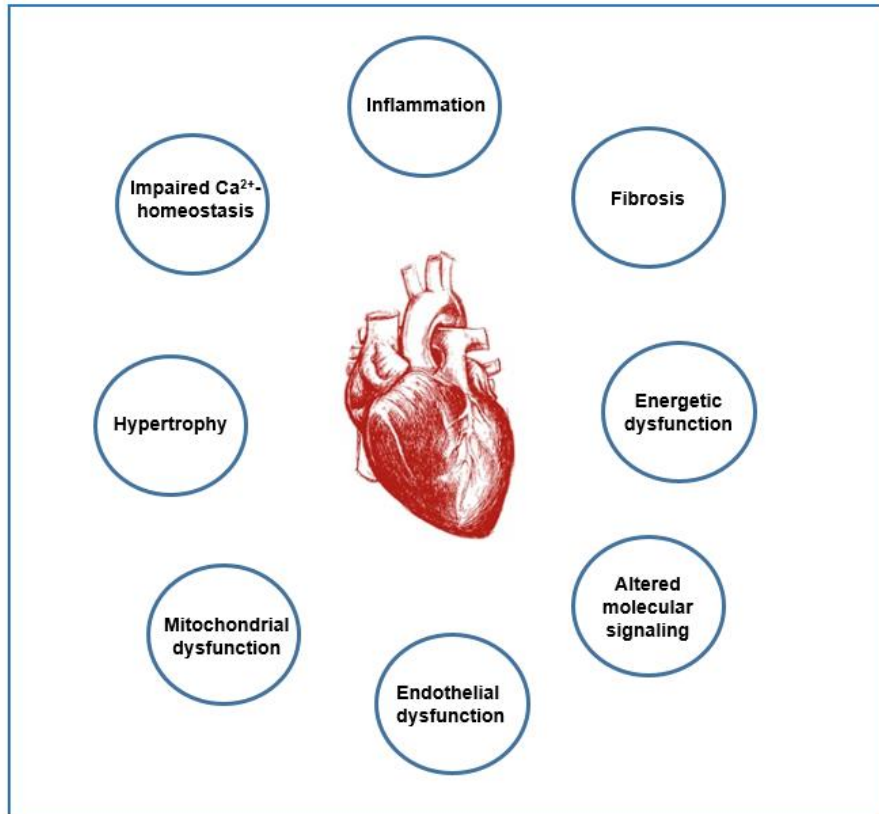
Figure 1: Molecular mechanisms and age-dependent structural and functional changes of the heart.

1.2 Signaling pathways regulating cardiovascular aging

Deregulation of growth and nutrient signaling pathways, including the mammalian target of rapamycin (mTOR) and insulin-like growthfactor-1 (IGF-1) signaling, play an important role in age-related cardiac hypertrophy and functional decline of the cardiovascular system.

1.2.1 Mammalian target of rapamycin (mTOR)

mTOR is a serine-threonine protein kinase responsible for the insulin and growth factor signaling as well as sensing of intracellular nutrient levels, regulation of cell size, growth, survival and proliferation as well as protein synthesis and gene transcription [6]. mTOR exists as two functionally distinct multi-protein signaling complexes, namely mTORC1 and mTORC2. The phosphoinositide-3-kinase (PI3K)/Akt/mTOR signaling pathway (Figure 2) is critical for cellular aging as the inhibition of this pathway extends the lifespan of many species (e.g. yeast, flies and worms) [26]. For instance, inhibition of the mTOR signaling pathway in Drosophila attenuates age-related decline in cardiac function [27]. Conversely, studies in the

mouse model, carrying cardiac-specific deletion of tuberous sclerosis complex 1 (TSC1), an upstream inhibitor of mTORC1 (mTOR complex 1), showed increased mTOR signaling in these mice, which developed dilated cardiomyopathy and had lower average lifespan [28]. Taken together, the activation of mTORC1 leads to protein translation and cell growth, whereas inhibition reduces growth and induces stress response pathways [29]. Binding of rapamycin, a natural fungicide substance that was isolated from the bacterium *Streptomyces hygroscopicus* is [30], to mTORC1 inhibits mTOR signaling pathway and decreases mTOR activity. A reduction of mTOR signaling by the rapamycin supplementation or via caloric restriction is linked to the induction of beneficial effects in the aged heart [31–33]. In contrast, chronic activation of the mTOR signaling cascade causes cardiac hypertrophy, fibrosis and decreased cardiac contractility [34].
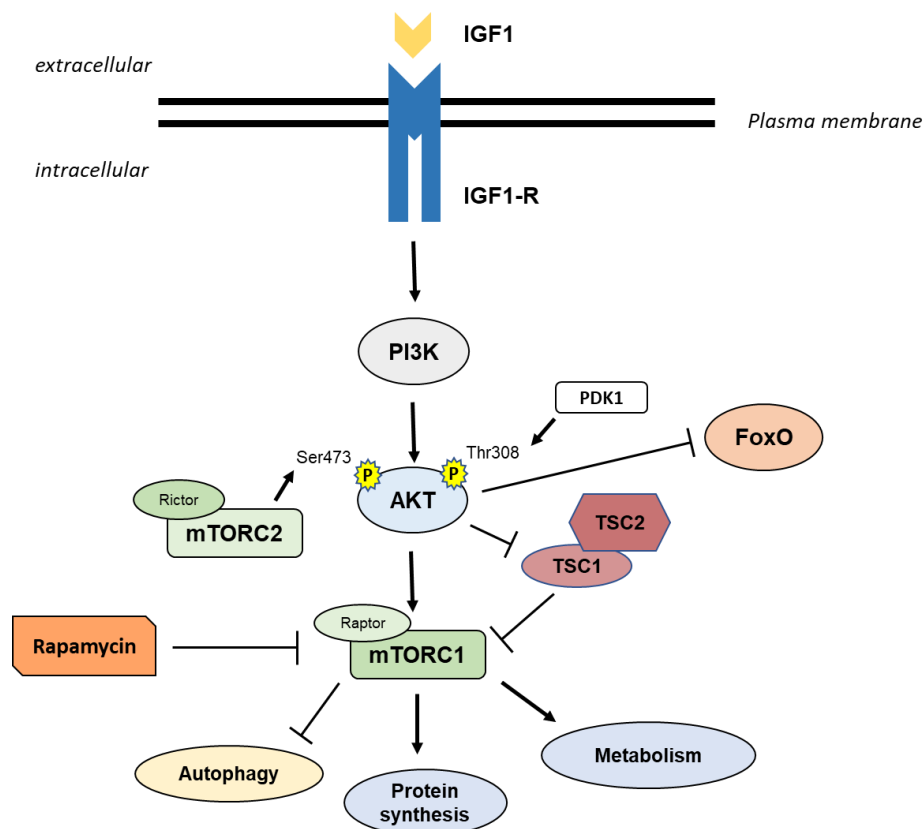
Figure 2 Schematic overview of the IGF-1/PI3K/Akt signaling pathways. IGF-1 binds to its receptors (IGF-1R) and activates the PI3K pathway. In turn, PI3K activates 3-phosphoinositide-dependent protein kinase-1 (PDK1), which then activates the downstream effector Akt at the phosphorylation site Thr308. mTORC2 stimulates mTORC1 activation by phosphorylation of Akt at the residue Ser473. Akt then phosphorylates tuberous sclerosis complex 2 (TSC2), and TSC2 binds and forms a complex with TSC1. TSC1/-TSC2 complex inhibits activation of mTORC1. Activation of mTORC1 leads to protein synthesis, metabolism and inhibition of autophagy. Rapamycin inhibits mTORC1 by binding to Raptor. Phosphorylation of FoxO by Akt is inhibitory. Abbreviations: IGF-1, insulin-like growth factor 1; PI3K, phosphatidylinositol-3 kinase; Akt, serine/threonine protein kinase; mTOR, mammalian target of rapamycin; FoxO, Forkhead box O; PDK1, 3-phosphoinositide-dependent protein kinase-1; mTORC, mTOR complex; TSC, tuberous sclerosis complex.

1.2.2 IGF-1/PI3K pathway

Insulin-like growth factor 1 (IGF-1) signaling cascade (Figure 2) is one of the most studied and best characterized longevity pathways. The IGF-1 signaling pathway exerts pleiotropic effects on many cellular functions, such as growth and differentiation as well as tissue repair [35–37]. Furthermore, IGF-1/PI3K signaling is implicated in cardiac aging and longevity by regulating several cellular processes, including senescence, apoptosis and autophagy [38, 39]. Cardiac tissue produces IGF-1 in response to growth hormone (GH) stimulation. IGF-1 binding to the IGF-1 receptor (IGF-1R) leads to further activation of downstream targets, including phosphoinositide 3-kinase (PI3K), a regulator of many physiological functions, such as cell growth and survival [40]. The complexity of this signaling pathway is underscored by controversial findings from different animal and human studies [41, 42].

There is a notable prolongation of longevity in several model organisms upon inhibition of the IGF-1 signaling pathway. Studies in fruit flies and mice showed improved cardiac performance and attenuated age-related dysfunction due to a deficient insulin/IGF-1 signaling [43, 44]. Cardiomyocyte-specific deletion of IGF-1R attenuates cardiac aging by reducing fibrosis and hypertrophy, whereas cardiac overexpression of IGF-1 stimulates collagen production and development of interstitial fibrosis and impaired systolic function [45].

Mice overexpressing IGF-1R specifically in the heart, develop physiological hypertrophy with no evidence of histopathology and enhanced systolic function at 3 months of age, which is maintained for up to 12-16 months of age [36]. In contrast, study by Delaughter *et al.* demonstrated that IGF-1 overexpression initially causes physiological hypertrophy and enhanced systolic function, which progresses to a pathological form of hypertrophy and increased left ventricular fibrosis with advanced age. In the elderly, age-dependent decline in IGF-1serum levels correlates with an increased risk of development of heart failure [46, 47]. However the effect of IGF-1 on the lifespan and cardiac aging in humans remains unclear [47].

PI3K (including the catalytic subunit p110α) is activated upon IGF-1 binding to the IGF-1R and is known to be the critical effector downstream of IGF-1R. PI3K is responsible for the regulation of heart size and physiological growth, and there is a positive correlation between the activation of IGF-1/PI3K pathway and the development of physiological hypertrophy [48]. Mice harbouring cardiac-specific overexpression of IGF-1R have significantly increased activity of PI3K and its downstream target Akt [40]. IGF-1R overexpression-induced cardiac hypertrophy is completely blocked by the inhibition of PI3K activity, suggesting that IGF-1R promotes hypertrophy in a PI3K-dependent manner [36]. Mice with a constitutively active PI3K

activity (caPI3K) show enlarged hearts associated with increased size of cardiomyocytes and normal cardiac function as well as normal lifespan, whereas the dominant negative mice (dnPI3K) have smaller hearts and reduced cell size of cardiac myocytes along with preserved cardiac function and extended lifespan [49].

1.2.3 Downstream targets of IGF-1/PI3K signaling pathway

Akt

Akt (i.e. protein kinase B, PKB) is a serine/threonine kinase and is a downstream target of the PI3K signaling pathway (Figure 2) and an important determinant of physiological heart growth [50]. Akt stimulates protein synthesis via mTOR, while inhibits protein degradation via the transcription factors of the Forkhead-Box-Protein (FoxO) family [51]. Akt is activated through two phosphorylation sites, namely Thr308 (phosphorylated by phosphoinositide-dependent protein kinase 1 (PDK1)) and Ser473 (phosphorylated through a mechanism that involves mTOR complex 2 (mTORC2)), respectively [52, 53]. Studies in mice with a constitutive overexpression of Akt demonstrated increased cell size, hypertrophy and interstitial cardiac fibrosis [54].

Forkhead-box-proteins (FoxO)

The Forkhead box protein family of transcription factors are downstream effectors of Akt (Figure 2), which play an important role in cell metabolism, proliferation, cell cycle control and aging in several cell types [55]. FoxO proteins also mediate stress response through transcription of genes involved in oxidative stress, metabolism, autophagy, aging, and apoptosis [56].

The activity of FoxOs is regulated by PI3K-mediated activation of Akt, which phosphorylates FoxO and creates a 14-3-3 binding site, that masks the nuclear localization signal (NLS), leading to nuclear export. In the cytosol FoxO is sequestered by 14-3-3 proteins and is in an inactive form. In the absence of negative regulation by Akt, FoxO factors remain in the nucleus, where they induce transcription of several downstream target genes that induce inhibition of proliferation and induce cell cycle arrest [55, 57, 58]. On the one hand, mice with loss of FoxO1 function are embryonically lethal, while mice with the loss of FoxO3a appear normal at birth, but they develop heart failure and cardiac hypertrophy later in life. On the other hand,

overexpression of FoxO1 or FoxO3 inhibits cardiac hypertrophy in cultured cardiomyocytes [59, 60]. Activated FoxO3 stimulates lysosomal proteolysis in different cell types by inducing the expression of autophagy-related genes, thus activating autophagy. [61–63].

1.3   Autophagy

Autophagy, or the process of cellular "self-eating" is an evolutionary conserved mechanism essential for the maintenance of cellular homeostasis, protein quality control and cell survival [64]. The role of autophagy is to degrade dysfunctional and damaged, potentially toxic cytoplasmic components, organelles, protein aggregates or lipid vesicles, and thus to protect cells against the accumulation of cellular waste and damage. Autophagy also promotes the recycling of cellular nutrients, which enables cells to survive during starvation. Once macromolecules have been degraded, monomeric units are exported to the cytosol for reuse and are made available for further anabolic processes [65, 66]. Autophagy-related genes (ATGs), encode 41 Atg proteins [67] that are essential during the autophagosome-biogenesis, which consist of several steps, including pre-autophagosome nucleation, elongation of the autophagosomal membrane, and genesis of autophagolysosome. Multiple protein complexes are involved in the different stages of autophagosome biogenesis, which can be categorized into different groups according to their functions at the various events within the autophagy pathway [68, 69]. There are different forms of autophagy, namely macroautophagy (herein referred to as autophagy), microautophagy and chaperone-mediated autophagy (CAM). Autophagy begins with the sequestration of cytoplasmic components designated for degradation by enclosure of an isolation membrane (i.e. phagophore) that forms an autophagosome, which fuses with a lysosome to form an autolysosome (Figure 3). Such engulfed material within autophagosomes is enzymatically degraded by lysosomal hydrolases [70]. In the process of microautophagy, cytoplasmic components are directly engulfed by invagination of the lysosomal or late endosomal membrane, whereas in the chaperone-mediated autophagy process substrates for degradation are labeled by the five-amino acid sequence (KFERQ or Lys-Phe-Glu-Arg-Gln). This sequence is recognized by heat shock proteins (Hsc70), which directly translocate the labeled cargo across the lysosomal membrane through a multimeric translocation complex called lysosomal-associated membrane protein 2A (LAMP2A) [66, 71].
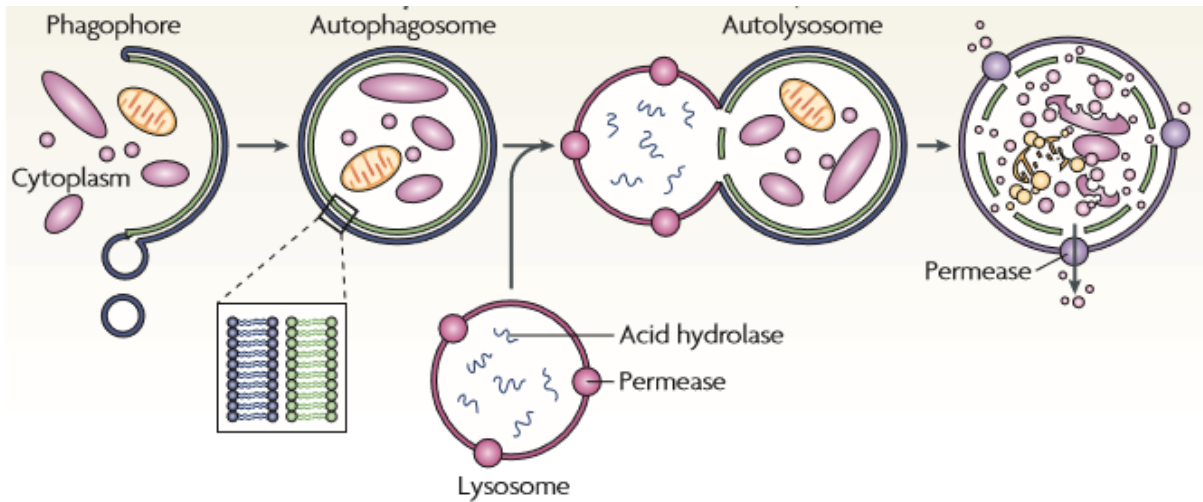
Figure 3: Process of autophagy. Cytoplasmic components are enclosed by an isolation membrane (i.e. phagophore) that expands to a double-membrane autophagosome. The membrane fusion between autophagosomes and lysosomes forms autolysosome, which contain acid hydrolases and permeases. This leads to the degradation of the cytoplasmic cargo and the lysosomal membrane. The degraded macromolecules are released through permeases and recycled in the cytoplasm. Reprinted from: [70]

Basal level of autophagy is a quality control mechanism that exists in virtually all cells. Its purpose is to ensure cellular homeostasis under normal conditions via clearance and degradation of long-lived or misfolded proteins, toxic protein aggregates or damaged organelles. However, an activation of the autophagy machinery is triggered by different stressors, including nutrient deprivation, hypoxia or pathogen infection [69].

On the one hand, autophagy can be non-selective, for example under starvation, when any part of the cytoplasm is self-digested in order to provide nutrients and so maintain cellular functions. On the other hand, autophagy can work highly selective by degrading targeted cargoes, such as specific protein aggregates, mitochondria, peroxisomes, endoplasmic reticulum or bacterial pathogens [66, 70]. In contrast to non-selective autophagy, the selective form recognizes selective autophagy receptors (SARs) that label cargo and directs it for specific degradation [72, 73]. The best characterized type of selective autophagy is the degradation of damaged mitochondria or mitophagy. During aging or under stress conditions, like hypoxia, damaged mitochondria have to be removed from the cytoplasm before they initiate and cause cell death [74].

1.3.1 Signaling pathways regulating autophagy

The eukaryotic cells react to nutrient depletion, stress or insufficient supply of growth factors by the inhibition of growth and induction of autophagy. The AMP-activated protein kinase (AMPK) and mTOR are two major short-term energy sensors essential for the rapid regulation of autophagy [75]. Although the mechanisms underlying the age-associated decline in autophagy have not been fully elucidated, it is conceivable that the longevity pathways contribute to such reduction in autophagy. Hyperactivation of mTOR [76–78] as well as reduced AMPK activity [79–81] in old age can directly inhibit autophagy (Figure 4). Moreover, age-related changes in the longevity signaling pathways contribute to the transcriptional regulation of autophagy as exemplified by the negative regulation of FoxO transcription factor family during aging due to (i) reduced AMPK activity [82], (ii) Akt-mediated phosphorylation [83] and (iii) lysin acetylation resulting from SIRT-1 deactivation [84, 85]. This negative transcriptional regulation can, in turn result in reduced expression of autophagy genes in the heart.
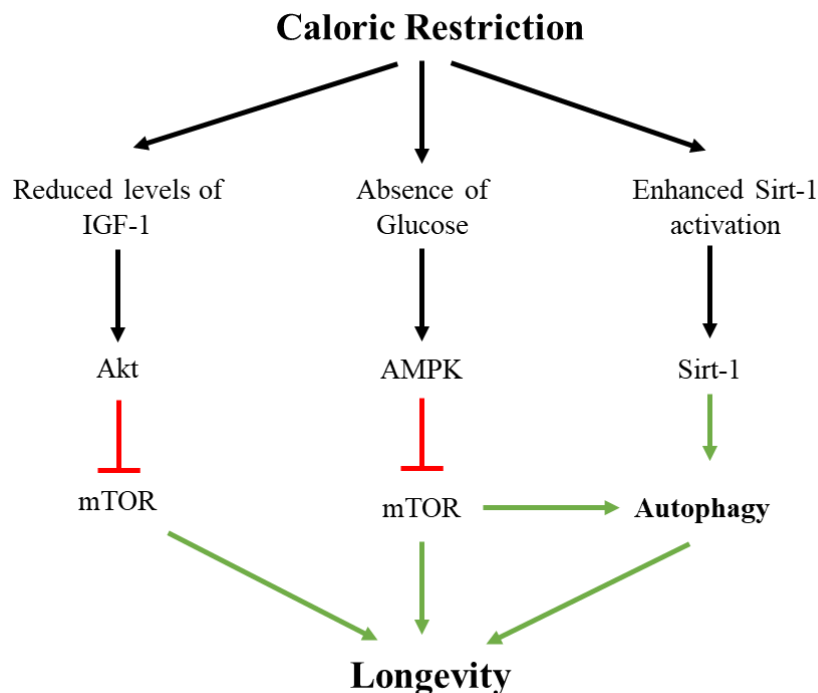
Figure 4 Signaling pathways in the regulation of autophagy. Nutrient starvation by caloric restriction exerts beneficial effects on autophagy signaling, and thus on longevity. Reduced levels of IGF-1 and energy sources (e.g. glucose) cause inhibition of mTOR signaling due to reduced Akt phosphorylation or increased AMPK activity. Enhanced activation of Sirt-1 upon caloric restriction induces autophagy and promotes longevity. Abbreviations: IGF-1 – Insulin-like growth factor 1, m TOR – Mammalian target of rapamycin, AMPK - AMP-activated protein kinase, Sirt-1 – Sirtuin 1.

IGF-1 longevity signaling pathway is known to regulate autophagy and its inhibition exerts beneficial effects on lifespan [86, 87]. It has been reported, that IGF-1 blocks autophagy via the activation of its downstream target Akt, what leads to further activation of mTOR, which is known to negatively regulate autophagy [88, 89]. Additionally, IGF-1 deficiency during nutrient deprivation increases cardiac AMPK activity. An inhibitory effect of IGF-1 on autophagy has been observed in mice, suggesting that reduced IGF-1 signaling results in enhanced autophagy [88]. Troncoso *et al.* showed that IGF-1 inhibits autophagy by increasing ATP levels, which leads to reduced AMPK activation in cultured cardiomyocytes [89]. These findings were confirmed in mice overexpressing a dominant negative AMPK activity, which manifested reduced autophagy [90]. Taken these results together, the inhibitory effect of IGF-1 on autophagy is based on stimulation of the IGF-1R/Akt/mTOR axis and inhibition of AMPK activity [91].

1.3.2   Autophagy in cardiac aging

Age-associated cardiac dysfunction is related to the accumulation of toxic proteins and dysfunctional, damaged cell components, including organelles and protein aggregates, in cardiomyocytes [92, 93]. Therefore, the degradation of such long-lived proteins and organelles via autophagy is a key mechanism to maintain cardiac tissue homeostasis over the course of aging. Recent studies show that impaired autophagy is coupled to cardiac hypertrophy under several pathological stimuli, indicating that intact autophagic machinery is indispensable for the maintenance of functional and structural homeostasis of the aging heart [75, 94].

The role of autophagy in cardiac aging is demonstrated by various animal models, in which the autophagy process has been manipulated via tissue-specific inactivation of autophagy-related genes. For example, cardiac-specific deletion of autophagy-related-gene *Atg5* in mice results in cardiac dysfunction, including myocardial hypertrophy, impaired contractile function, accumulation of collapsed mitochondria, enhanced oxidative stress, cardiac fibrosis and consequently, shortened lifespan [95]. Mice with a global deficiency of lysosome-associated membrane protein-2 (LAMP-2), a protein responsible for proper fusion between autophagosome and lysosome, show increased accumulation of autophagic vacuoles and impaired degradation of long-lived proteins, which leads to cardiac hypertrophy and contributes to development of cardiomyopathy [96]. Dysfunction of autophagy, in particular the selective form (e.g. mitophagy) is linked to several age-related maladies [97, 98], including

cardiovascular diseases [74], implying that autophagy is an essential biological process affecting cardiac health and aging.

1.3.3 Induction of Autophagy by the Caloric Restriction Mimetic Spermidine

A growing body of evidence suggests that autophagy is downregulated with age [99]. Hence, interventions to increase the level of autophagy may slow or even prevent the progression of aging in the heart (Figure 5).
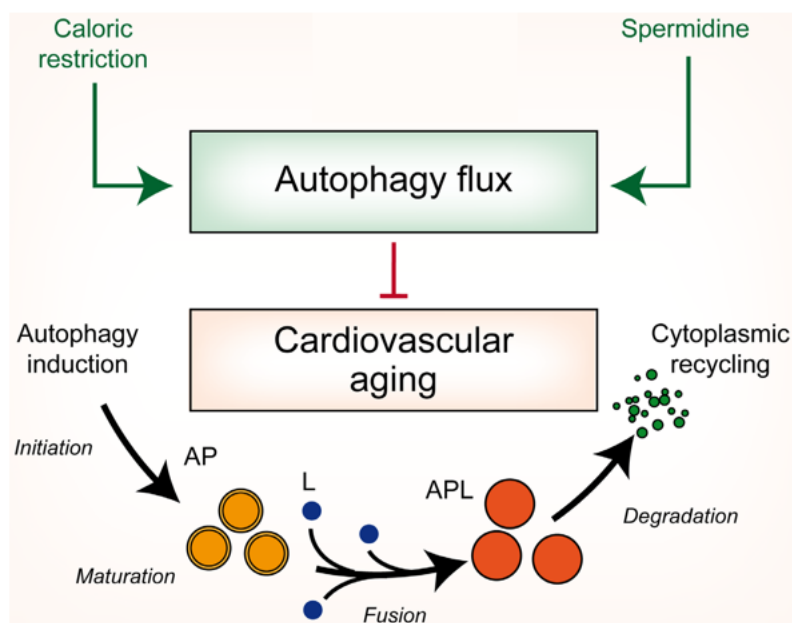
Figure 5: Supplementation of spermidine induces autophagy and prevents the progression of cardiac aging. Activation of autophagy by nutritional or pharmacological interventions slows down cardiovascular aging and thereby promoting longevity in several model organisms. AP indicates autophagosome; APL, autophagolysosome; and L, lysosome. Reprinted from: [74]

Caloric restriction (CR), defined as the chronic reduction of calorie intake without malnutrition, is so far the only proven dietary regimen, that extends the lifespan and has beneficial health effects in several tested model organisms [7, 100]. Yet, the implementation of CR is difficult, if not impossible, for people to stick with and adopt into their lifestyle in the long term. However, another attractive feasible strategy is an increased intake of caloric restriction mimetics (CRMs). These agents imitate beneficial metabolic effects of dietary or caloric restriction by inducing autophagy through deacetylation of cytosolic and nuclear proteins [101]. One such CRM is a potent autophagy inducer and the naturally occurring polyamine spermidine, whose plasma concentration declines during aging in model organisms [102] as

well as in humans [103, 104]. Spermidine belongs to the polyamines (e.g. spermine and putrescine), which are ubiquitous polycationic molecules, involved in several important cellular processes, including cell growth, differentiation and proliferation, regulation of translational processes and apoptosis. Polyamines bind to DNA, RNA and phospholipids and regulate protein synthesis and stability. Changes in polyamine levels occur in many diseases (e.g. muscle related disorders [105], different types of cancer [106], cardiovascular disease [107]). Thus, the maintenance of normal polyamine levels is essential for a wide variety of fundamental cellular functions. Spermidine is important for cell survival and has anti-inflammatory and anti-oxidative properties [108, 109]. Spermidine is considered to be an effective intervention against cardiac aging [107]. Spermidine can be synthetized either from ornithine or methionine (Figure 6). Beside the endogenous cellular biosynthesis of spermidine, there are two other important sources of spermidine: (i) increased oral intake from different spermidine-rich dietary sources, such as fermented and matured cheeses, soy beans, lentils, green peas, nuts, certain mushrooms and wheat germ, and (ii) commensal polyamine-producing bacteria, which are responsible for the production of spermidine in the intestine of different species. Subsequently spermidine is absorbed in the gut by intestinal epithelial cells, and is further distributed to organs through systemic circulation [108, 110, 111]. The regulation of spermidine catabolism is mediated through acetylation and subsequent oxidation reactions catalysed by a set of specific enzymes.

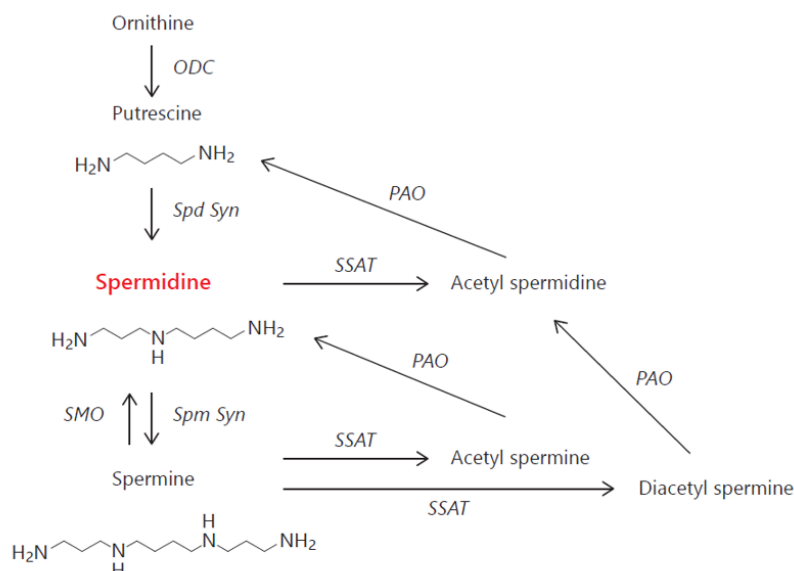**Figure 6**: **Polyamine metabolism.** Biosynthesis of the polyamine spermidine is regulated by the rate-limiting-step enzyme ODC: Spermidine is formed from its precursor putrescine or by degradation of spermine. Abbreviations: ODC - Ornithine decarboxylase; PAO - polyamine oxidase; SMO - spermine oxidase; Spd Syn - spermidine synthase; Spm Syn - spermine synthase; SSAT - spermidine/spermine N 1 -acetyltransferase. Reprinted from: [108]

1.3.4 Cardioprotective effects of spermidine

A recent study showed that spermidine ameliorates age-associated cardiac dysfunction and prolongs lifespan of old mice [107]. Indeed, spermidine supplementation via drinking water had cardioprotective effects by reducing age-related cardiac hypertrophy, preserving diastolic function, improving mitochondrial respiration and enhancing cardiac autophagy as also mitophagy. Spermidine feeding also reduced myocardial passive stiffness by increased titin phosphorylation and suppressed subclinical inflammation (Figure 7). The beneficial cardioprotective effects of spermidine supplementation are not reproduced in mice with incompetent autophagy in the heart. Indeed, aged mice deficient for autophagy-related protein *Atg5* in cardiomyocytes develop diastolic dysfunction and hypertrophy upon spermidine supplementation, indicating that autophagy underlies spermidine-induced cardio-protection. In salt-sensitive Dahl rats, an experimental model for hypertension-induced heart failure, spermidine treatment preserves diastolic function, reduces systemic blood pressure, prevents cardiac hypertrophy and decreases myocardial stiffness, thus preventing the onset of cardiac dysfunction, which is observed in non-treated control rats. In humans, a correlation exists between increased spermidine uptake and prevention of cardiovascular disease as, lower incidence of heart failure correlates with higher levels of dietary spermidine. In view of the cytoprotective role of autophagy and mitophagy, these results indicate that supplementation of spermidine is a promising and feasible strategy delaying the onset of cardiovascular disease [107, 112, 113].
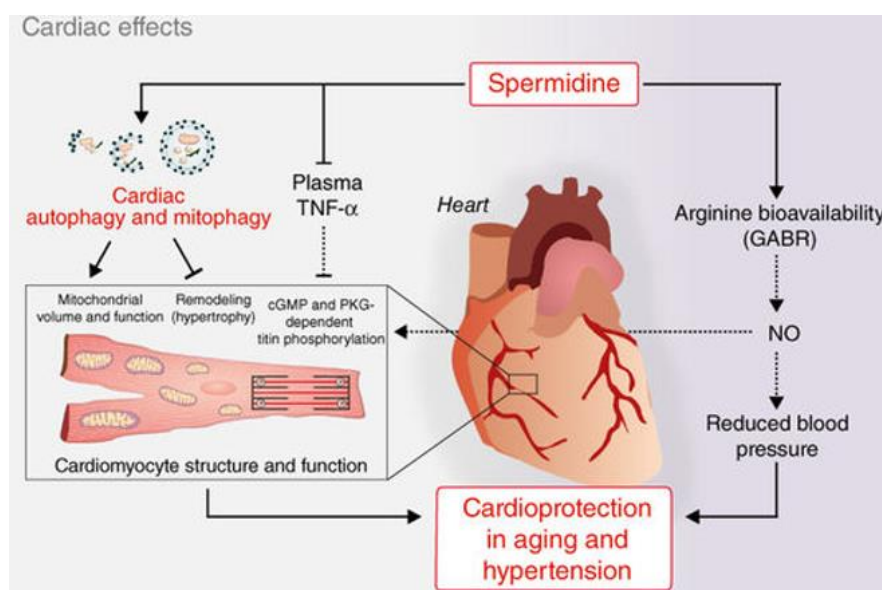

Figure 7 Spermidine-mediated cardioprotection in aging and hypertension. Oral supplementation of spermidine improves cardiac function by the induction of autophagy and mitophagy in cardiac tissue, reducing inflammation, lowering systemic blood pressure and improving mechano-elastical properties of cardiomyocytes. Reprinted from: [107]

1.4 Previous studies leading to this work

Several studies showed a negative correlation between increased IGF-1 plasma levels and lifespan [114, 115], implying that the serum level of circulating IGF-1 serves as marker for the progression of aging. IGF-1 signaling affects the intracellular calcium homeostasis, contractility, metabolism, autophagy, hypertrophy, aging and apoptosis [38, 39].

The downregulation of IGF-1 signaling pathways by several dietary or genetic interventions has been shown to improve health and prolong life span in model organisms including mice [43, 44]. Interestingly, IGF-1 signaling has both beneficial and deleterious effects on age-related diseases influencing lifespan. For instance, downregulation of the IGF-1 pathway protects against several metabolic alterations that promote cardiovascular disease [43]. In line with this findings, the inhibition of the PI3K/Akt signaling pathway protects the heart from cardiac aging [116]. On the contrary, reduced IGF-1 levels correlate with a decline in cardiac contractility and diastolic function and the progression of cardiovascular disease [117]. Our preliminary results show that 12-month-old cardiomyocyte-specific IGF-1R overexpressing mice have significantly better left ventricular ejection fraction and increased left ventricular hypertrophy (i.e. increased wall thickness and heart weight) compared to WT mice. Interestingly, despite improved ejection fraction with respect to WT mice, IGF-1R mice show comparable stroke volume and comparable cardiac output. These results indicate, that IGF-1-R mice exhibit diastolic dysfunction (low diastolic volume) as manifested by left ventricular (LV) decreased diastolic filling rate, which is compensated by increasing contractility to sustain stroke volume and workload in order to maintain sufficient ejection fraction. Increasing arterial stiffness leads to a compensatory mechanism by the myocardium, including LV hypertrophy and cardiac remodeling. These findings suggest that IGF-1R mice develop diastolic dysfunction earlier in their old age compared to WT animals. A recent study showed that spermidine inhibits the PI3K/Akt signaling pathway and that PI3K as an important downstream target of IGF-1R inhibits polyamine synthesis (including spermidine) [118]. This indicates an interaction between spermidine and the IGF-1/PI3K signaling network. A recent study by Chrisam *et al.* showed that the induction of autophagy by spermidine in skeletal muscle from WT mice involves decreased Akt phosphorylation [105].

1.5 Aim of this work and hypothesis

The major aim of this work was, to elucidate whether cardioprotective effects by spermidine are mediated, at least partially, through the IGF-1/PI3K/Akt signaling pathway (Figure 8). To

this end, we tested the hypothesis, that oral spermidine supplementation or intraperitoneal injections of spermidine, inhibits the IGF-1/PI3K/Akt signaling pathway in the mouse heart.

Assessment of the downstream targets of the IGF-1 signaling, such as phosphorylation status of Akt protein (e.g. Thr308 and Ser473) and mTOR in spermidine-treated hearts by immunoblotting will prove or dismiss the hypothesis that spermidine induces autophagy through inhibition of PI3K/Akt activity in IGF-1R mice.

Immunoblotting was also used to assess changes in the expression and phosphorylation of key transcription factor (FoxO3a). These experiments are expected to reveal, which of the IGF-1 downstream targets is critical for cardioprotective effects by spermidine.
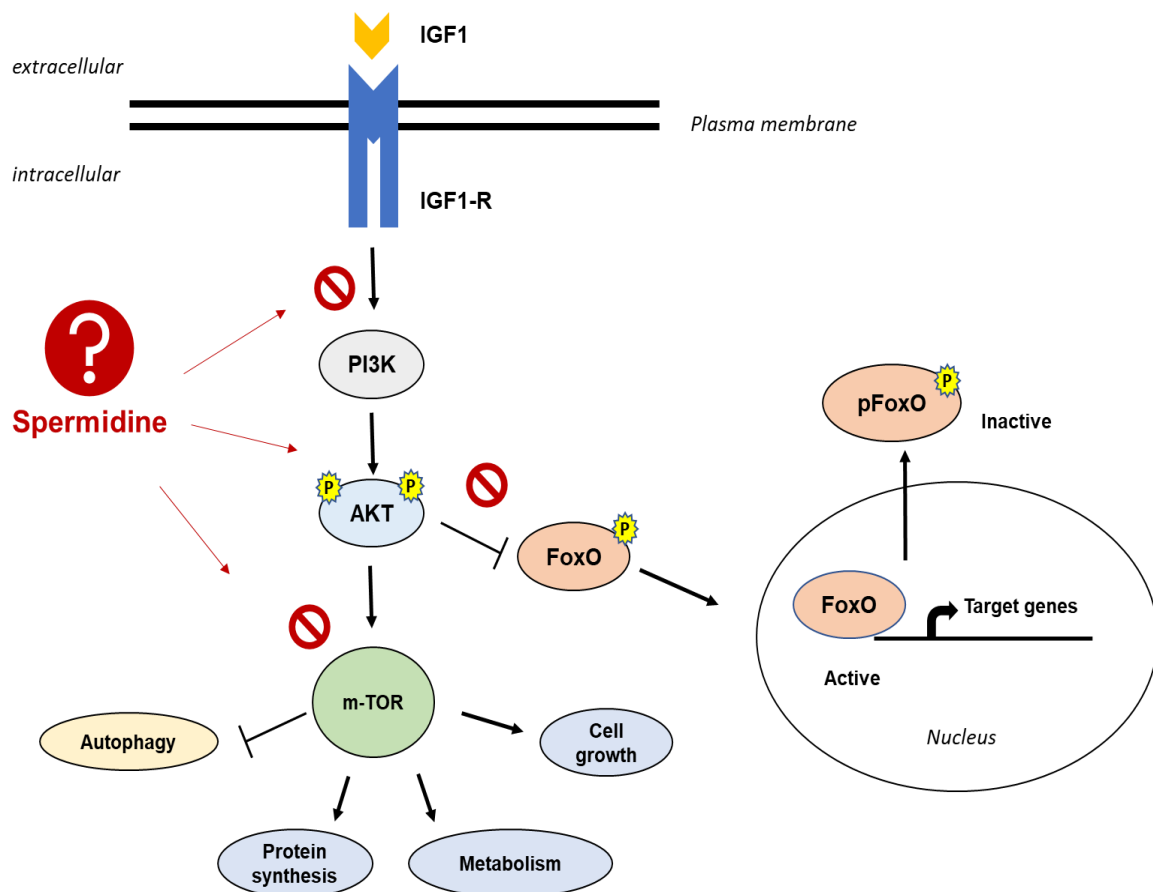
Figure 8 Our working model and hypothesis: Spermidine inhibits the IGF-1/PI3K/Akt signaling pathway in the heart. Binding of IGF-1 to plasma membrane IGF-1 receptor (IGF-1R) mediates phosphatidylinositol-3kinase (PI3K) activation and Akt phosphorylation, which are inhibited by spermidine. Inactivation of the PI3K/Akt pathway inhibits downstream targets (e.g. mTOR) and activates autophagy. Furthermore PI3K/Akt signaling inhibition reduces the phosphorylation of FoxO transcription factors, leading to nuclear import and activation of transcriptional activity of Atg-related genes. Abbreviations: IGF-1, Insulin-like growth factor 1; PI3K, Phosphatidylinositol-3 kinase; Akt, Serine/threonine protein kinase; mTOR, Mammalian target of rapamycin; FoxO, Forkhead box O.

2   Materials and Methods

2.1   Mice

<u>IGF-1R</u>

In this study, we used 12-month-old male mice overexpressing cardiomyocyte-specific insulin-like growth factor-1 receptor (heterozygous IGF-1R mice). These mice were generated in the laboratory of Prof. Seigo Izumo, Beth Israel Deaconess Medical Center and Harvard Medical School, as follows: the cDNA insert for human IGF-1R was cloned into a SalI-digested MHC promoter construct. This vector contains a 5.8 kb BamHI-MaeIII fragment of murine αMyHC (alpha-myosin heavy chain) gene that includes the promoter and exons 1-3 from the 5´untranslated region of the gene, as well as the human growth hormone polyadenylation site. These animals show up to 20-fold increase in the expression of the IGF-1R specifically in the heart, while IGF-1 plasma levels are not elevated [36]. Age-matched wild type (WT) littermates (FVB/N strain) served as controls. Genotype was determined from ear biopsies by PCR-based analysis using the following primers: IGF-1R forward: αMHC-4: 5'GGC ACT TTA CAT GGA GTC CT3' (LOT-Nr.: 2355627, Microsynth), reverse: IGFR-1R: 5'GAA CAG CAG CAA GTA CTC GGT AAT3' (LOT-Nr.: 2355628, Microsynth).

<u>dnPI3K</u>

Heterozygous adult male mice harbouring cardiomyocyte-specific inhibition of phosphoinositide 3-kinase (dominant negative PI3K mice – dnPI3K) were used at 5-10 months of age. Also, these mice were generated in the laboratory of Prof. Seigo Izumo as described elsewhere [50]: Briefly, the cDNA insert for Ish2p110 or p110 kinase gene was cloned into a SalI-digested α-MyHC promoter construct. This vector contains a 5.8 kb BamHI-MaeIII fragment of the murine α-MyHC gene that includes the promoter and exon 1-3 from 5´untranslated region of the gene, as well as the human growth hormone polyadenylation site. These transgenic animals show around 20% of PI3K activity [49]. Age-matched wild type (WT) littermates (FVB/N strain) served as controls. Genotype was determined from ear biopsies by PCR-based analysis using the following primers: dnPI3K forward: αMHC-4: 5'GGC ACT TTA CAT GGA GTC CT3' (LOT-Nr.: 2355627, Microsynth), reverse: p110-2R: 5'TGGCCTCTCTGAACAGTTCAT3' (LOT-Nr.: 2355626, Microsynth).

The total number of animals used in these experiments was 102 mice, therefore 78 mice were from the IGF-1-R strain and 24 mice from the dnPI3K cohort. All animal procedures were performed in accordance with national and European ethical regulation and approved by the government agencies (Bundesministerium für Wissenschaft, Forschung und Wirtschaft, BMWFW, Austria, animal permissions: BMWFW-66.010/0160-WF/V/3b/2014 and BMWFW-66.010/0198-WF/V/3b/2017).

2.2   Animal housing

Mice were housed in temperature-controlled animal facilities under specific-pathogen-free (SPF) or conventional conditions in 12 h light/dark cycles. All mice had access to food (standard chow-diet, Cat. Nr. V1534-703, Ssniff, Germany) and drinking water *ad libitum.*

2.3   Spermidine supplementation

Chronic spermidine treatment

Male mice were randomly divided into 4 groups according to the genotype and treatment (Figure 9). Supplementation of 3 mM spermidine (SPD) (Cat. Nr. S2626, Sigma-Aldrich, USA) was administered orally via drinking water, starting at the age of 7 months for 5 months. Control animals received regular drinking water.
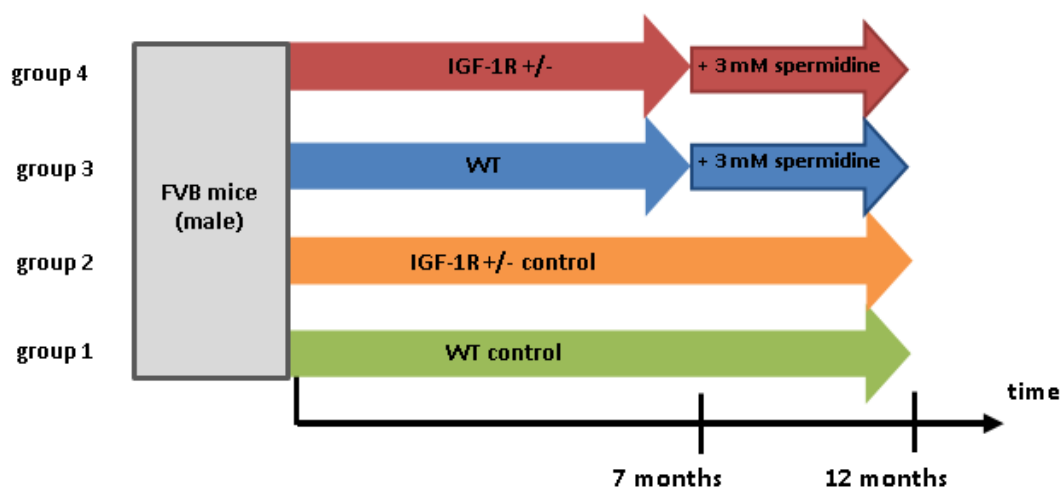
Figure 9: Schematic overview of experimental design and chronic spermidine administration. IGF-1R and WT mice were randomly divided into SPD-treated and control groups. Spermidine treatment (3 mM spermidine into drinking water) started at the age of 7 months for 5 months. Abbreviations: WT – wilde-type, IGF-1R – Insulin-like growth factor-1 receptor, SPD - spermidine, mM - millimolar

Acute spermidine treatment

Young (5-10 months old) IGF-1R and dnPI3K mice as well as their WT littermates were subjected to intraperitoneal (i.p.) injection of either spermidine (50 mg/kg BW, dissolved in 0.9% NaCl) or 0.9% NaCl (control, vehicle). Sixteen to twenty-four hours after i.p. injections animals were anesthetized using 5% isoflurane and euthanized using cervical dislocation. The organs were immediately removed as described below (see 2.5 Organ harvesting). Male mice were randomly divided according to the treatment and genotype (Figure 10).
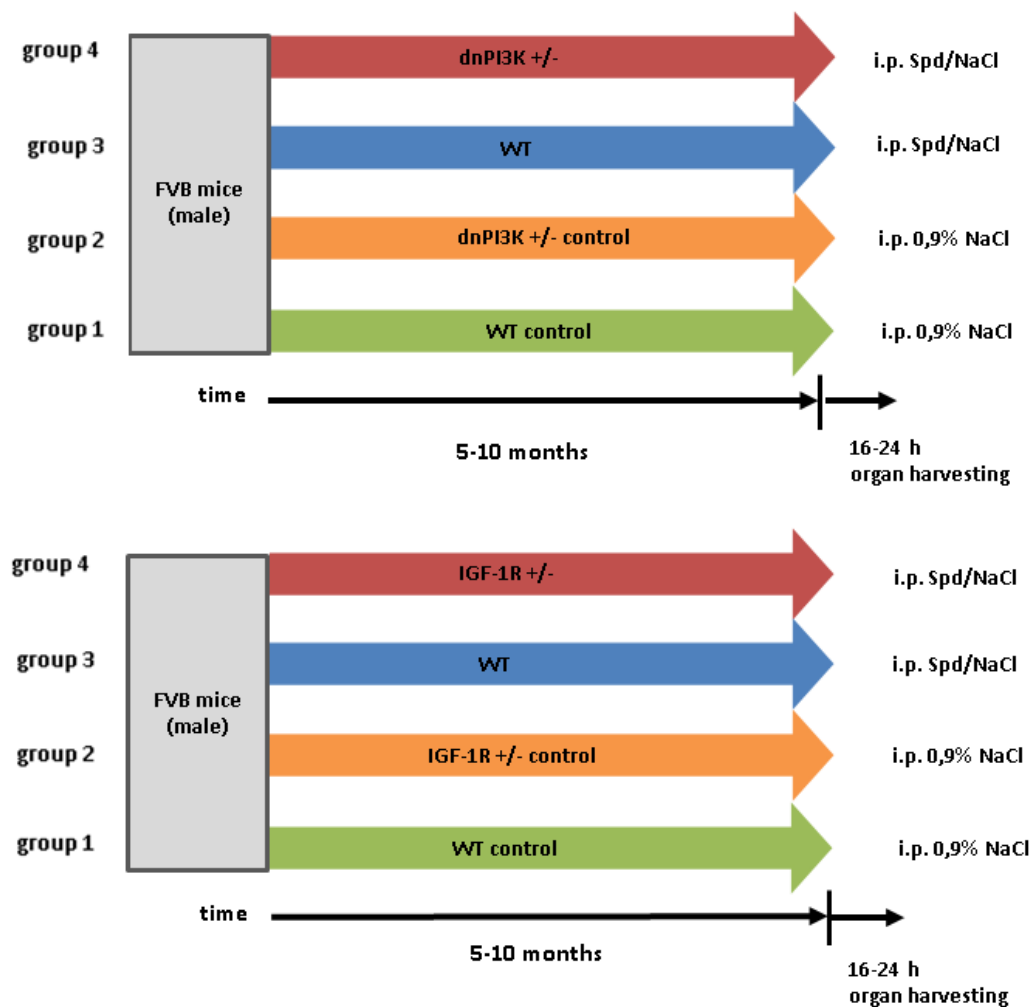

Figure 10: Schematic overview of experimental design and acute spermidine administration. Young (5-10 months) IGF-1R, dnPI3K and WT mice were randomly divided according to treatment and genotype into 4 groups. Abbreviations: WT – wilde-type, IGF-1-R – Insulin-like growth factor-1 receptor, dnPI3K – dominant negative phosphoinositide 3-kinase, SPD - spermidine, mM - millimolar

2.4 Spermidine preparation

Spermidine stock solution (1M) was prepared on ice as follows: spermidine free base (pH of approximately 13) was dissolved in sterile ice-cold and deionized H_2O. Then pH was adjusted to 7.3 by adding 37% HCl (Cat. Nr.320331, Sigma-Aldrich, USA) dropwise, while the solution was continuously stirred on ice. Titration with 37% HCl is an exothermic reaction that releases heat, which may negatively affect the stability of spermidine. Spermidine stock solution was sterile filtered (filter system 0.2 µm, Cat. Nr. 156-4020, Thermo Scientific Fisher Inc., USA), aliquoted and stored at -20°C. Aliquots were used within 3 months to avoid spermidine deamination.

2.5 Organ harvesting

After the hemodynamic assessment, animals (at the age of 12 months) were euthanized and blood was collected by apical puncture of the heart. Organs (heart, lung, liver, spleen, kidney, white adipose tissue) were quickly collected, rinsed in PBS and weighed. Hearts and other organs were immediately dissected, immersed into ice-cold 2-methylbutane (Cat. Nr. 106056, Merck Millipore, USA) for a few seconds and then flash frozen in liquid nitrogen. The samples were stored at -80°C until they were further processed.

2.6 Tissue preparation and protein extraction

Immunoblotting was performed from whole heart lysates. For protein extraction, cardiac tissue was disrupted using a pre-cooled mortar and pestle. Pieces of frozen myocardium (around 30 mg) were added to 100 µl cold lysis buffer (see Table 1). Myocardial tissues were grinded by using a small potter until they were completely homogenized. Then the lysates were centrifuged at 5000 rpm for 3 minutes at 4°C. The supernatant was collected in a pre-cooled 1.5 ml safe-lock tube (Cat. Nr. 0030120.086, Eppendorf, Germany). The pellet was resuspended in 100 µl lysis buffer and added to the supernatant. Tubes containing the homogenate were centrifuged at 14.000 rpm for 5 minutes at 4°C. The supernatant was transferred to a new collection tube and the lysates were snap-frozen in liquid nitrogen and stored at -80°C. A small amount of homogenate was used for further determination of protein concentration using bicinchoninic acid (BCA) assay.

Table 1: Composition of lysis buffer for the homogenization of the cardiac tissue

Lysis Buffer composition	
Concentration	Substance
1%	NP 40 (IGEPAL CA-630)
10%	Glycerole
137mM	NaCl
20 mM	Tris-HCl pH = 7,4
20 mM	NaF
1 mM	Sodium orthovanadate
1 mM	Sodium pyrophosphate
50 mM	β-Glycerophosphate
10 mM	EDTA pH = 8
1 mM	EGTA pH = 7
4 µg/ml	Aprotinin
4µg/ml	Leupeptin
4µg/ml	Pepstatin
1 mM	PMSF

2.7   Determination of protein concentration – BCA assay

To determine protein concentrations of the whole tissue lysates the BCA assay (BCA-Assay, Cat. Nr. 23227, Thermo Fisher Scientific Inc., USA) was employed. For this purpose, a calibration curve was generated using 7 standards of different Bovine Serum Albumin (BSA, Cat. Nr. A7906, Sigma-Aldrich, USA) concentrations ranging from 0.5 µg/µl to 3.0 µg/µl.

Three different dilutions of tissue lysates, each with an end volume of 10 µl, were prepared for the measurement. BCA working reagent (500 µl, 50 parts A + 1 part B) was added to each lysate dilution and BSA standard and gently mixed prior these samples were incubated in the water bath for 20 min at 37°C. Photometric measurement (BioPhotometer, Eppendorf, Germany) was performed at the end of the incubation time. Absorbed light by blank (only lysis buffer as a reference), BSA standards and tissue lysate dilutions was then measured at wavelength of 562 nm. Finally, protein concentration of each sample was calculated based on the BSA standard calibration curve.

2.8 Western Blot

The immunoblot or Western Blot is used for the detection of specific proteins and their quantitative expression. This method allows to test for the presence of a single protein, which can be detected from whole tissue homogenate. Protein separation is based on molecular weight and performed by sodium dodecyl sulfate polyacrylamide gel electrophoresis (SDS-PAGE). Separated proteins are then transferred on a nitrocellulose or PVDF membrane, which is then incubated along with a specific antibody. Binding of the labeled antibody enables visualization of the target protein.

2.8.1 SDS-PAGE

Protein samples (40 µg) were used for measurements of protein levels by SDS-PAGE. XT sample buffer (6.25 µl of 4x buffer, Cat. Nr. 1610791, Bio-Rad, USA) and XT reducing agent (1.25 µl of 20x agent, Cat. Nr. 1610792, Bio-Rad, USA) were added to the sample. Lysis buffer was added to reach a total volume of 25 µl per sample. The samples were gently mixed and kept on ice. Electrophoresis chamber was filled with 400 ml of running buffer (20x XT MOPS, Cat. Nr. 1610788, Bio-Rad, USA). Samples (25 µl each) and protein standards (8 µl each, Precision Plus Protein™ All Blue Standards, Cat. Nr. 1610373, Bio-Rad, USA), which served as a standard for the determination of molecular weight of protein bands in subsequent immunoblotting analyses were added to 4-12% Criterion™ XT Bis-Tris gels (Cat. Nr. 3450124, Bio-Rad, USA). Gels were run at 70 V and 120 V for 20 minutes and 2 hours, respectively (Figure 11).
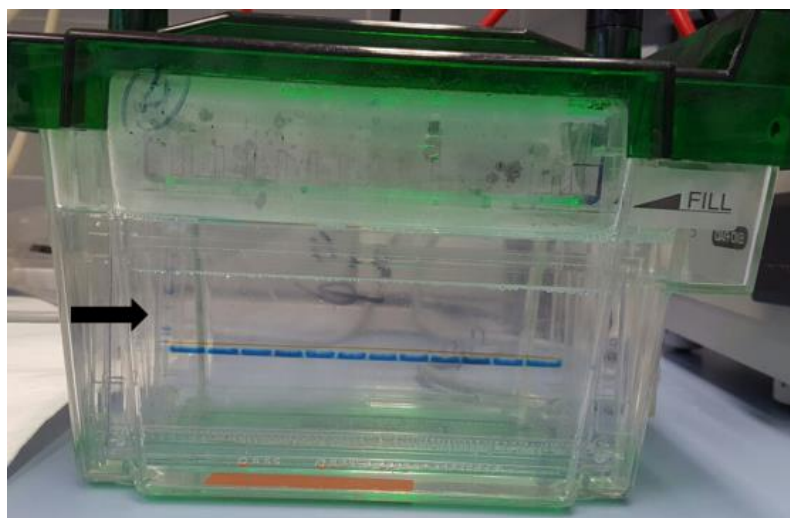

Figure 11: Electrophoresis chamber. Blue bands indicate different samples as well as 4 x sample buffer. Protein standard was added (see arrow on the left, Precision Plus Protein™ All Blue Standards) that served as a reference for the molecular weight of the proteins.

2.8.2 Transfer

After electrophoresis, proteins were transferred onto 0.45 µm nitrocellulose membranes (Cat. Nr.10600002, GE Healthcare Life science, UK). To this end, transfer buffer (6.5mM Tris, 38.4mM Glycine, 20% Methanol) and filter papers (Gel Blot Paper GB003, Cat. Nr. 732-4229, VWR, USA) were prepared, while the membranes and sponges were equilibrated in the buffer before assembling the blotting sandwich (Figure 12).

Figure 12: Western Blot transfer cassette setup for the wet transfer. Assembling order from top to bottom: sponge – filter paper – gel – nitrocellulose membrane – filter paper – sponge. For the wet transfer, the gel side of the sandwich is oriented toward the cathode (black), while the membrane side is positioned toward the anode (red).

The blotting cassette was then placed in a transfer tank (CriterionTM Blotter, Cat. Nr. 1704071, Bio-Rad, USA) filled with the transfer buffer. The tank was connected to the power supply and the transfer was run at 400 mA for 2 hours at 4°C. The whole setup was placed on ice during the blotting.

To test whether the transfer was successful, membranes were stained with Ponceau S solution (Cat. Nr. P7170, Sigma-Aldrich) for 10 minutes. This staining allows to visualize protein bands on the membrane (Figure 13). Before de-staining the membranes with ddH$_2$O, copies of them were made for documentation. Then the membranes were cut in stripes according to the size of each protein. After the washing step in 1 x TBST (10 mM Tris/HCl, pH 7.5, 150 mM NaCl, 0.1% Tween-20), the membranes were blocked with the blocking solution (5% non-fat dry milk [w/v] (Cat. Nr. T145.2, Carl Roth, Germany) in 1x TBST) and incubated for 1 hour at room temperature. This step is necessary to block any unspecific protein-binding sites on the membranes.
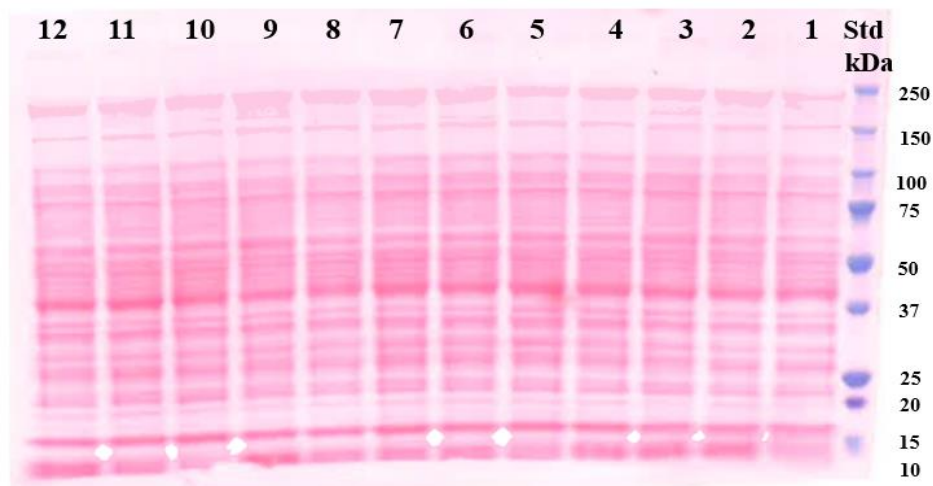
Figure 13: Ponceau S staining of nitrocellulose membrane. Membrane was incubated for 10 minutes at room temperature in Ponceau S solution, to label protein bands and then washed with ddH2O. Red bands show proteins from different samples in the slots 1-12. Protein standard was added to the right side of the membrane. Molecular weights were within 10 kDa and 250 kDa.

2.8.3   Immunodetection

After the blocking step, membranes were washed in 1 x TBST for 10 minutes. Single membranes were incubated with primary antibody overnight at 4°C. All primary and secondary antibodies were diluted as indicated in Table 2 using 0.5% non-fat dry milk in 1xTBST. After being washed 4 times with 1xTBST for 8 minutes, membranes were incubated with horseradish peroxidase-conjugated secondary antibodies on a shaker for 35 min at room temperature. The primary antibodies that were used are listed in Table 2 and the secondary antibodies are listed in Table 3.

Table 2: List of primary antibody dilutions

Primary antibody	Size (kDa)	Company (Cat. Nr.)	Dilution
mTOR	289	Cell Signaling (#2972)	1:1000
IGF-1R	97	Santa Cruz (#sc-713)	1:500
Akt	60	Cell Signaling (#9272)	1:1000
p-Akt(Ser473)	60	Cell Signaling (#9271)	1:750
p-Akt(Thr308)	60	Cell Signaling (#9275)	1:750
GAPDH	37	Cell Signaling (#5174)	1:5000
FoxO3a	87	Cell Signaling (#2497)	1:1000
p-FoxO3a(Ser253)	97	Cell Signaling (#9466)	1:1000

Table 3: List of secondary antibodies and their dilutions

Secondary antibody	Company	Dilution
ECL^{TM} Anti-Rabbit IgG, HRP-linked whole Ab (from donkey)	GE Healthcare Life Sciences	1:5000
ECL^{TM} Anti- Mouse IgG, HRP-linked whole Ab (from sheep)	GE Healthcare Life Sciences	1:5000

After additional 4 washing steps each lasting 8 minutes, the membranes were incubated with enhanced chemiluminescent substrate (ECL) for the detection of horseradish peroxidase (HRP) activity from bound secondary antibodies, which were detected by SuperSignal® West Pico Chemiluminescent Substrat (Cat. Nr. 34080, Thermo Fisher Scientific Inc., USA), Clarity™ Western ECL Substrat (Cat. Nr. 1705061, Bio-Rad, USA), or for maximum sensitivity SuperSignal® West Femto Substrate (Cat. Nr. 34096, Thermo Fisher Scientific Inc., USA). Chemiluminescence signals were visualized using the ChemiDoc™ Touch System (Cat. Nr. 1708370, Bio-Rad, USA). Densitometric quantification of the blots was performed using the Image Lab V5.2 software (Bio-Rad, USA).

2.8.4 Membrane stripping

In order to break the antibody bonds and remove already bound antibodies, the membranes were stripped. This process enables to detect more than only one protein or its phosphorylated form on the same blot as typically both have similar size.

Then the membrane was incubated in stripping buffer (Restore^{TM} PLUS Western Blot Stripping Buffer, Cat. Nr. 46430, Thermo Fisher Scientific Inc., USA). Duration of the incubation was adjusted to the signal intensity, - stronger signals require longer duration of the membrane stripping (and vice versa). However, this can last up to 1 hour in order to avoid any protein removal. After stripping the membrane was washed in 1xTBST and incubated for several minutes followed by an additional block using 5% milk. Finally, the membrane was incubated with another primary antibody at 4°C overnight.

2.9 Statistical analysis

Factorial analysis of variance (ANOVA) was used to compare groups, thereby considering treatment and genotype as fixed factors and the gel as a random factor to correct for inter-gel variability. Pair-wise comparisons (Student's t-test, Welch's t-test or Mann-Whitney U test) were performed, whenever main effects or interaction were significant. When 3 groups were compared (in the IGF-1R young, that were adjusted to i.p. spermidine injections), ANOVA was used followed by Tukey's post-hoc test. Normality of residuals and equality of variance were confirmed using Shapiro-Wilk and Levene's tests, respectively. If these criteria were not met, data were log-transformed to meet the assumptions. Two-sided P value < 0.05 was considered significant. IBM SPSS statistics software (Version 23) was used to run the statistical analysis. Data are presented as bar graphs presenting means; error bars denoting standard error of the mean (SEM).

3 Results

3.1 Expression of IGF-1R in IGF-1R mice

We first sought to confirm that IGF-1R hearts have increased expression of IGF-1R as reported previously [36]. As expected, IGF-1R mice had significantly higher expression of IGF-1R than WT animals (P=0,0001; Figure 14). However, this increase was significantly larger in control IGF-1R mice compared to spermidine-treated IGF-1R mice (P=0,007). In contrast, spermidine treatment had an opposite (i.e. positive) effect on the expression of IGF-1R in WT group, although this did not reach statistical significance (P=0,06).
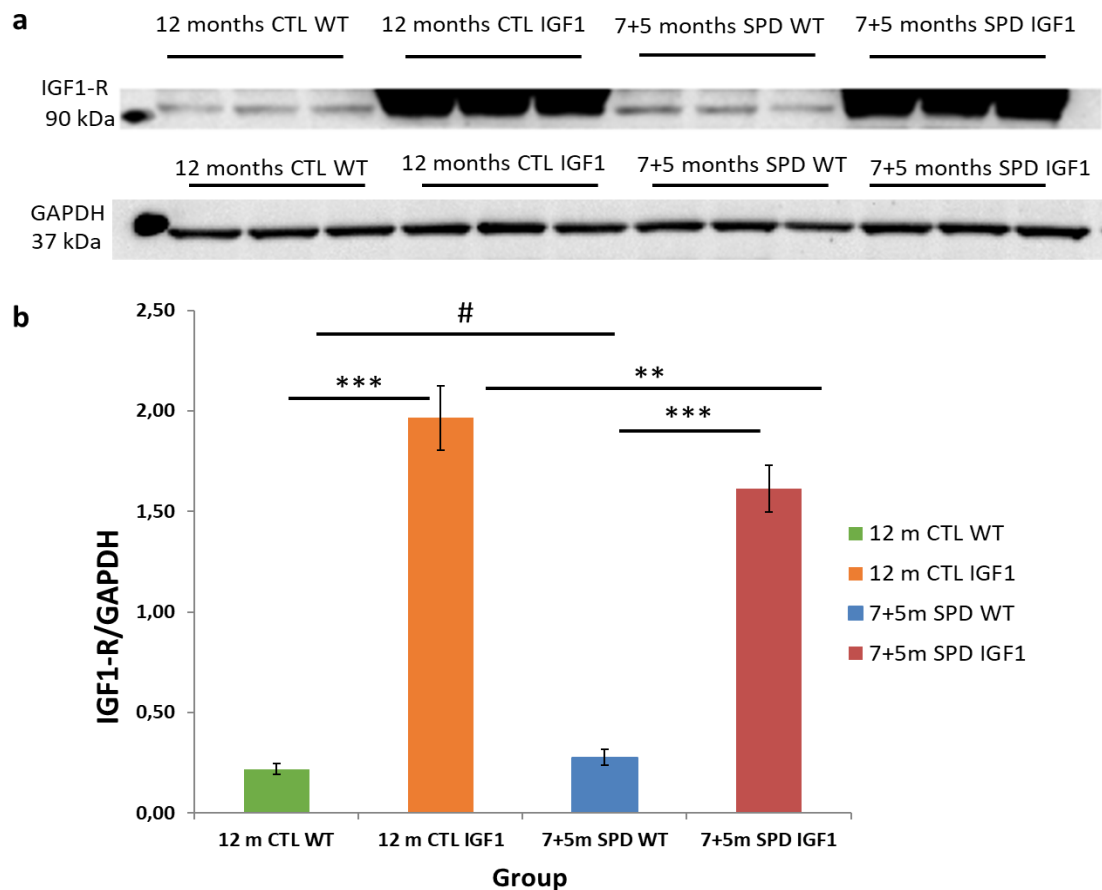
Figure 14: Expression of IGF-1R was reduced in IGF-1R mice by oral spermidine supplementation. a) Representative Western Blots show the expression of IGF-1R (90 kDa) and GAPDH (37 kDa) as a loading control. **b)** Western Blot analysis was done by densitometry. IGF-1R densitometric values were normalized to the loading control (GAPDH). N=15 mice/group. ***P<0.0001, *P<0.01, #P<0.06. Abbreviations: m - months, SPD – spermidine, CTL – control.

The IGF-1R is a receptor tyrosine kinase that is activated upon IGF-1 binding. The binding of IGF-1 to its receptor triggers the activation of several intracellular kinases, including the

activation of PI3K, which further stimulates downstream targets of the PI3K/Akt signaling pathway.

3.2 Akt expression in IGF-1R mice

IGF-1R overexpression in transgenic mice resulted in markedly reduced expression of Akt ($P=0,0001$ vs. WT mice). In addition, there was no effect or interaction between groups upon treatment with spermidine (Figure 15).

Figure 15: Expression of Akt was reduced in IGF-1R mice. a) . a) Representative Western Blots show the expression of Akt (60 kDa) and GAPDH (37 kDa) as a loading control. **b)** Western Blot analysis was done by densitometry. IGF-1R densitometric values were normalized to the loading control (GAPDH). N=15 mice/group. ***$P<0.0001$. Abbreviations: m - months, SPD – spermidine, CTL - control

3.3   Phosphorylation of Akt at Thr308 and Ser473 in IGF-1R mice

To test the activation level of Akt, we sought to determine the phosphorylation status of Akt protein at two residues, namely Thr308 and Ser473. The phosphorylation level of Akt at the Thr308 regulatory site (p-Akt-Thr308) was significantly increased in IGF-1R hearts with respect to WT hearts (P=0,0001; Figure 16). Spermidine treatment did not show any significant changes on the phosphorylation of Akt at Thr308 (Figure 16).
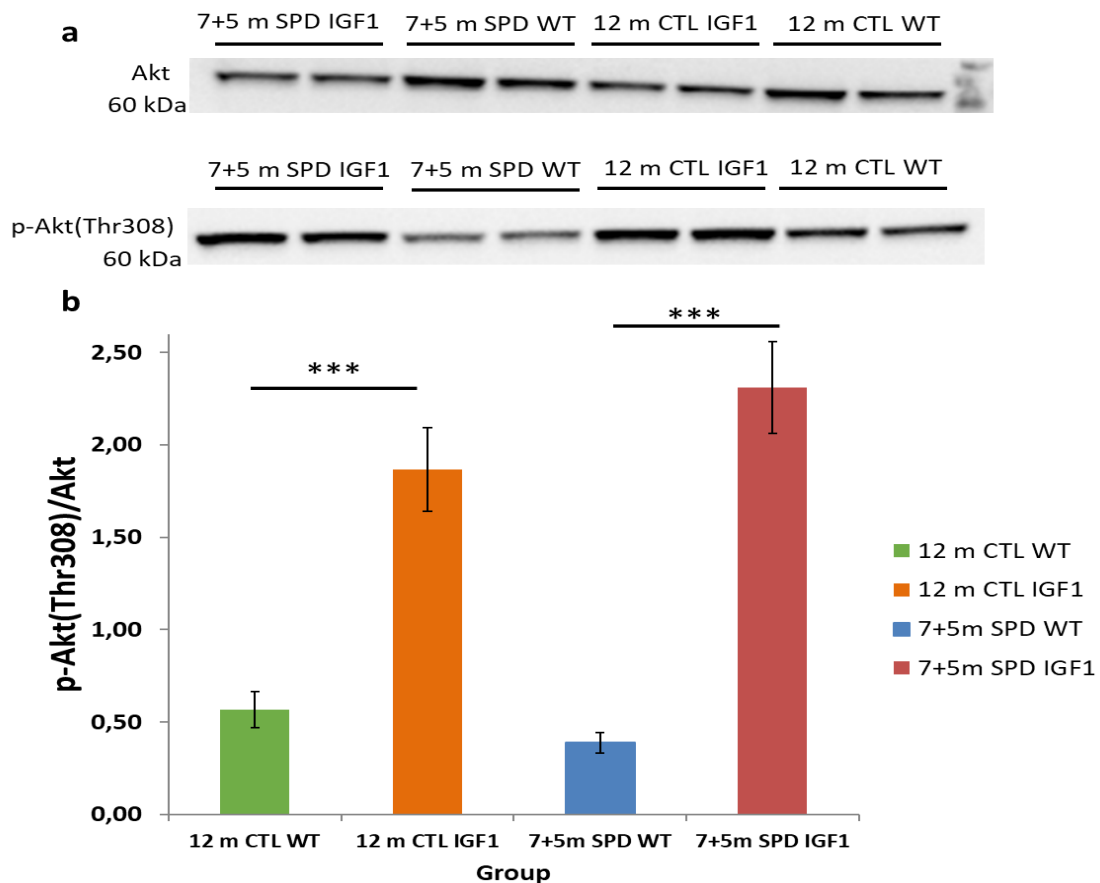
Figure 16: Akt phosphorylation at Thr308 is increased in IGF-1R mice a) Representative Western Blots show the phosphorylation of p-Akt(Thr308) (60 kDa) and total levels of Akt (60 kDa). **b)** The ratio of p-Akt(Thr308) to total expression of Akt was calculated after the quantification by densitometry. N=15 mice/group. ***P<0.0001. Abbreviations: m - months, SPD – spermidine, CTL - control

The phosphorylation of Akt at Ser473 site was significantly elevated in the IGF-1R mice (P=0,0001; Figure 17), and this increase was comparable between control and spermidine-treated hearts. However, we observed a strong trend for the reduction in phosphorylation upon supplementation of spermidine in WT hearts (P=0,052).
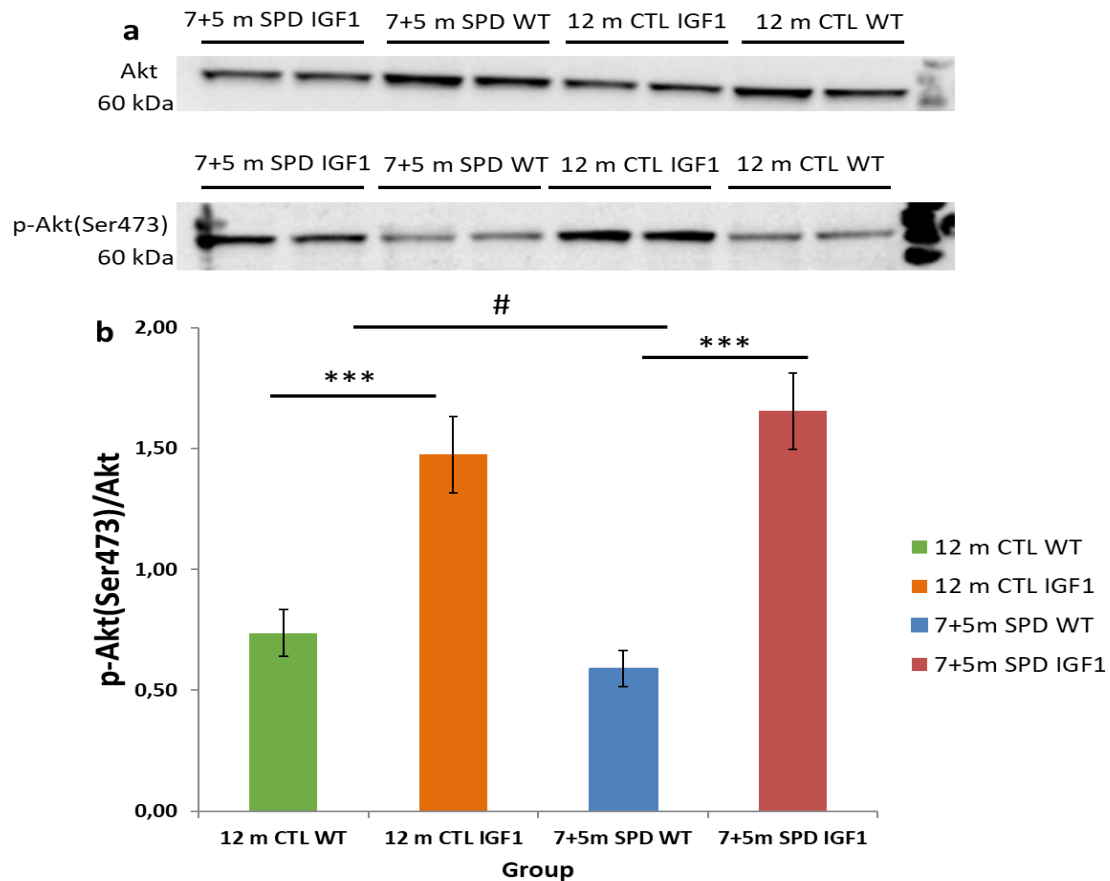
Figure 17: Akt phosphorylation at Ser473 was increased in IGF-1R hearts. a) Representative Western Blots show the phosphorylation of p-Akt(Ser473) (60 kDa) and total expression of Akt (60 kDa). **b)** The ratio of p-Akt(Ser473) to total expression of Akt (Akt) was calculated after the quantification by densitometry. N=15 mice/group. ***P<0.000; #P<0.06. Abbreviations: m - months, SPD – spermidine, CTL – control

Altogether, these results indicate that despite reduced Akt expression, the phosphorylation of Akt, and thus the activity of Akt is increased in IGF-1R mice.

3.4 Expression and phosphorylation of mTOR in IGF-1R mice

The expression of mTOR was comparable between WT and IGF-1R heart lysates and it was not affected by chronic spermidine supplementation (Figure 18).
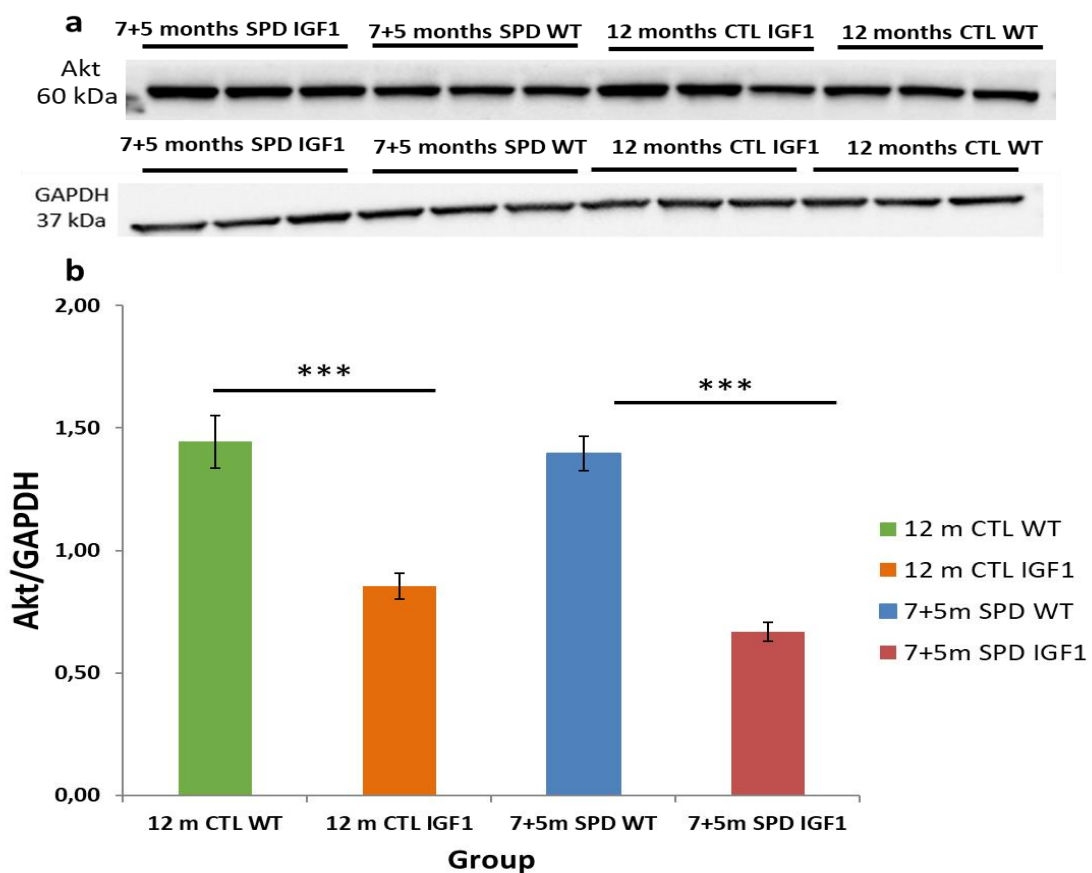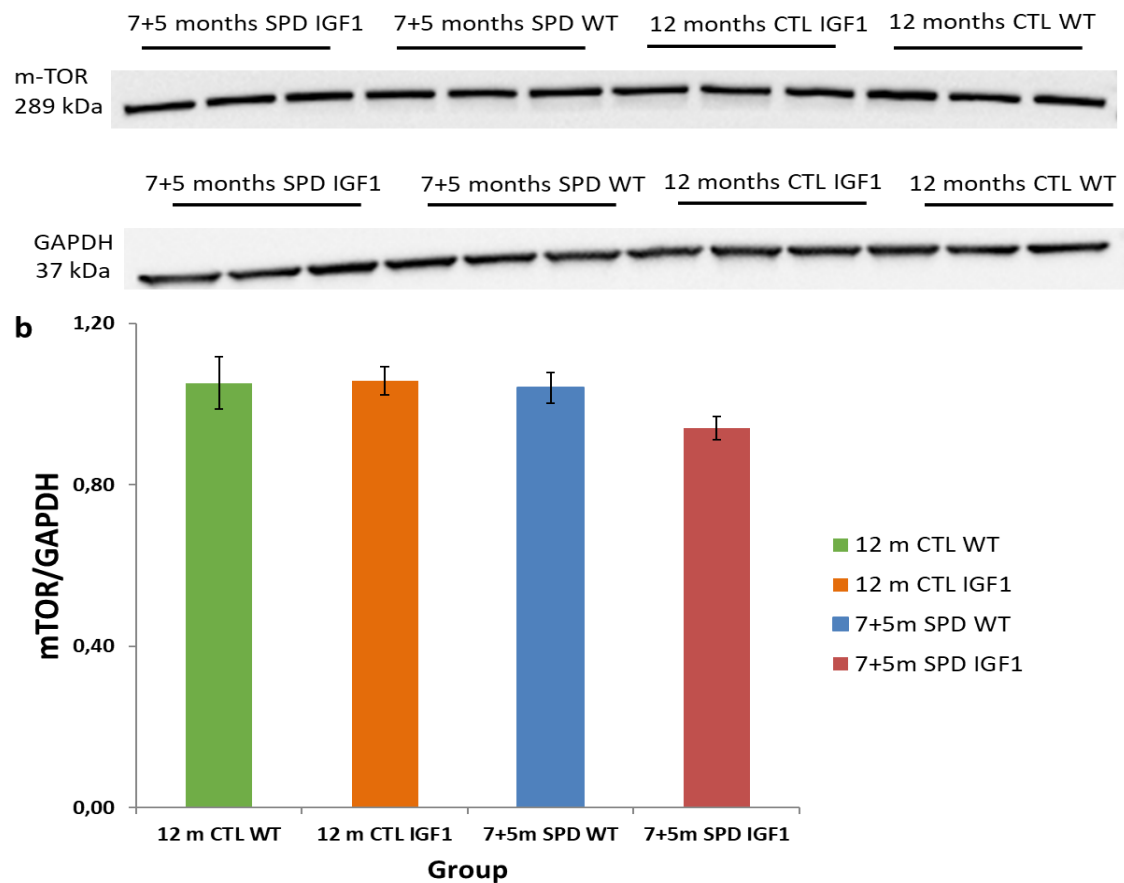
Figure 18: No differences in mTOR expression in IGF-1R mice. a) Representative Western Blots show the expression of mTOR (289 kDa) and GAPDH (37 kDa) as a loading control. **b)** Blots were quantified by densitometry and normalized to the loading control. N=15 mice/group. Abbreviations: m - months, SPD – spermidine, CTL – control

3.5 Akt expression in dominant negative PI3K mice phosphorylation

Next, we investigated the effect of reduced PI3K activity on downstream targets using dnPI3K mice, which were subjected to intraperitoneal injections of spermidine. This allowed us to assess for acute effects of spermidine compared to the chronical supplementation of spermidine (via drinking water). Expression of Akt was significantly increased in mice with dnPI3K compared to WT mice (P=0,0001). Spermidine treatment did not change the expression of Akt in none of the groups (Figure 19).
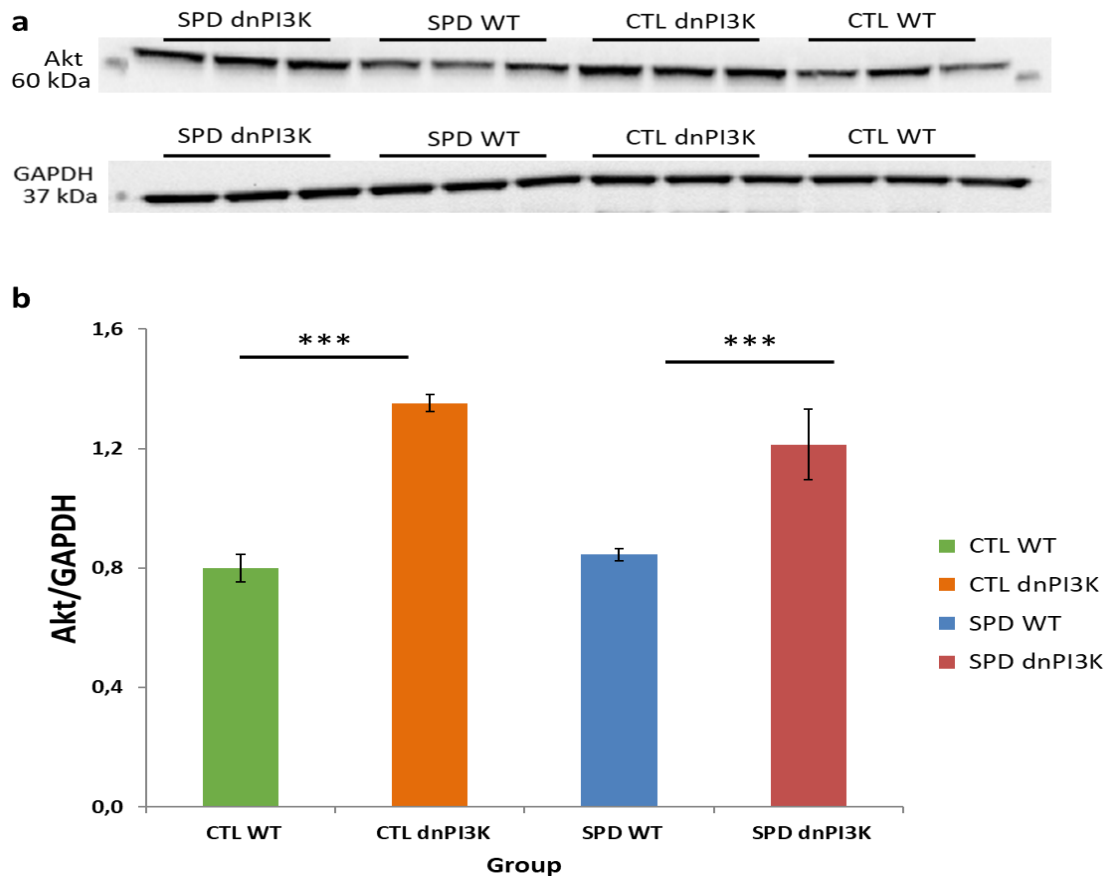
Figure 19: Expression of Akt was increased in dnPI3K mice. a) Representative Western Blots display expression of Akt (60 kDa) and GAPDH (37 kDa) as a loading control. **b)** Blots were quantified by densitometric method and normalized to the loading control. N=8 mice/group. ***P<0.0001. Abbreviations: m - months, SPD – spermidine, CTL - control

3.6 Akt phosphorylation in dnPI3K mice

Phosphorylation of Akt at Thr308 site was dramatically reduced in the dnPI3K mice compared to their WT littermates (P=0,0001; Figure 20). Acute spermidine treatment reduced p-Akt(Thr308) in WT group (P=0,023), but not in the dnPI3K cohort, which showed a trend toward increased p-Akt(Thr308). Spermidine administration also reduced the difference in Akt phosphorylation at the site Thr308 between WT and dnPI3K cohort (P=0,042), suggesting that spermidine, when applied acutely, acts via PI3K as the critical downstream effector of IGF-1R signaling pathway.
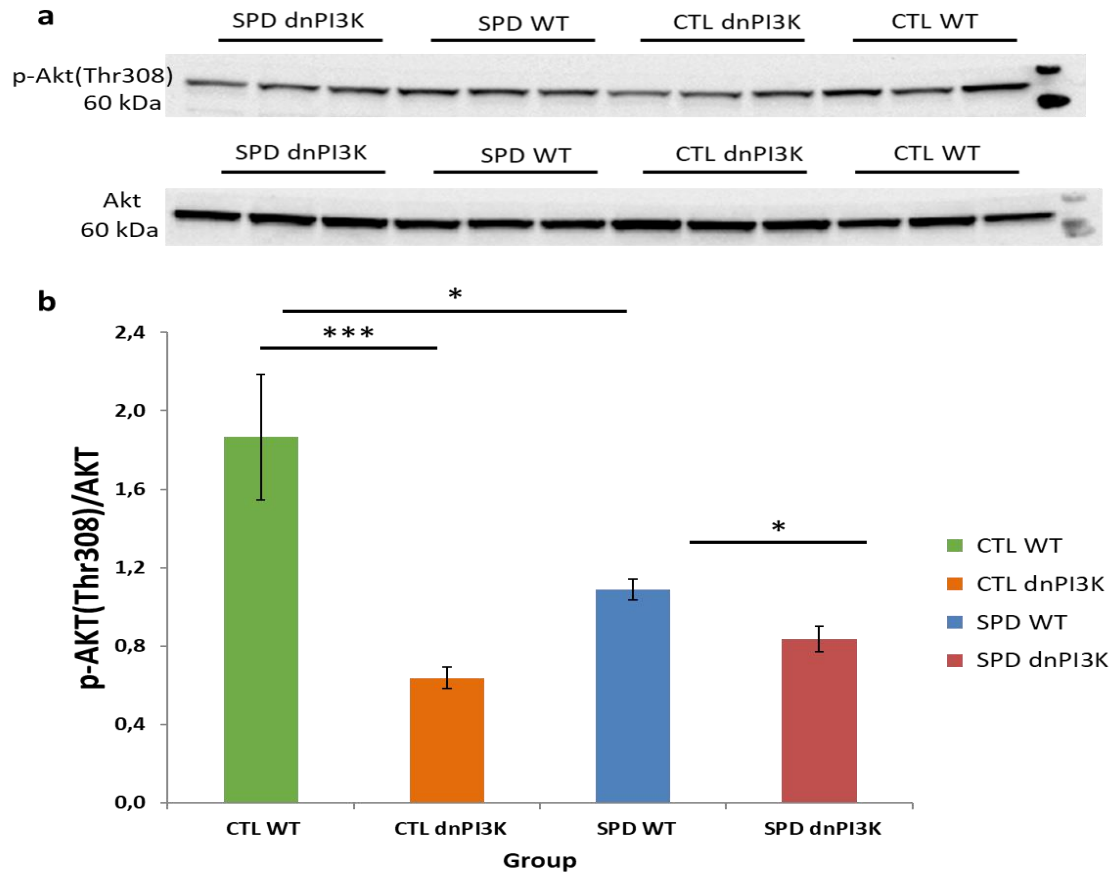
Figure 20: Phosphorylation of Akt at Thr308 was reduced in dnPI3K hearts. a) Representative Western Blots show p-Akt(Thr308) (60 kDa) and total expression of Akt (60 kDa). Treated groups (SPD) were subjected to i.p. injections of spermidine (50 mg/kg body weight SPD in 0.9% NaCl), whereas the control groups received injections of 0.9% NaCl **b)** The ratio of p-Akt(Thr308) to total Akt was calculated in 8 mice per group. ***P<0.0001, *p<0.05. Abbreviations: m - months, SPD – spermidine, CTL - control

To test whether these effects (on Akt phosphorylation at Thr308 site) can be recapitulated in IGF-1R mice, we subjected them to the intraperitoneal injection of spermidine as we did with dnPI3K animals.

Control IGF-1R mice had increased Akt activity as compared with age-matched WT littermates (P=0,049). Conversely, spermidine-treated IGF-1R mice showed comparable activity of the Akt pathway to that in WT controls (Figure 21).
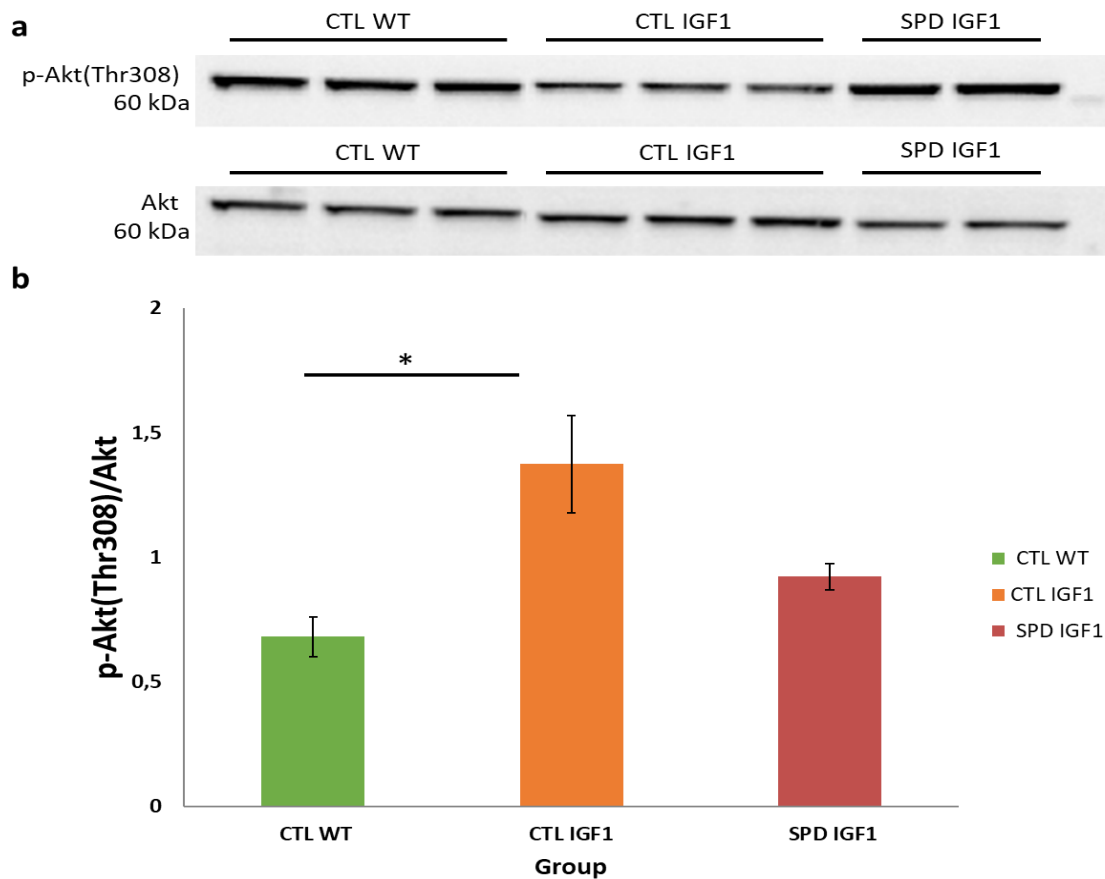
Figure 21: Phosphorylation of Akt at Thr308 was increased in young IGF-1R mice. a) Representative Western Blots show p-Akt(Thr308) (60 kDa) and total Akt expression. Treated groups (SPD) were subjected to i.p. injections of spermidine (50 mg/kg body weight SPD in 0.9% NaCl), whereas the control groups received injections of 0.9% NaCl. **b)** The ratio of p-Akt to total Akt (Akt) was calculated from 4-5 mice/group. *$P<0.05$. Abbreviations: m - months, SPD – spermidine, CTL - control

3.7 Akt phosphorylation of Ser473 site in dnPI3K mice

dnPI3K mice had significantly reduced Akt phosphorylation of Ser473 site compared to WT animals (P=0,0001; Figure 22). Interestingly, spermidine significantly increased Akt-Ser473 phosphorylation in the dnPI3K mice to control (baseline) levels from WT mice, which showed a trend toward an increased Akt-Ser473 phosphorylation upon spermidine administration (Figure 22).
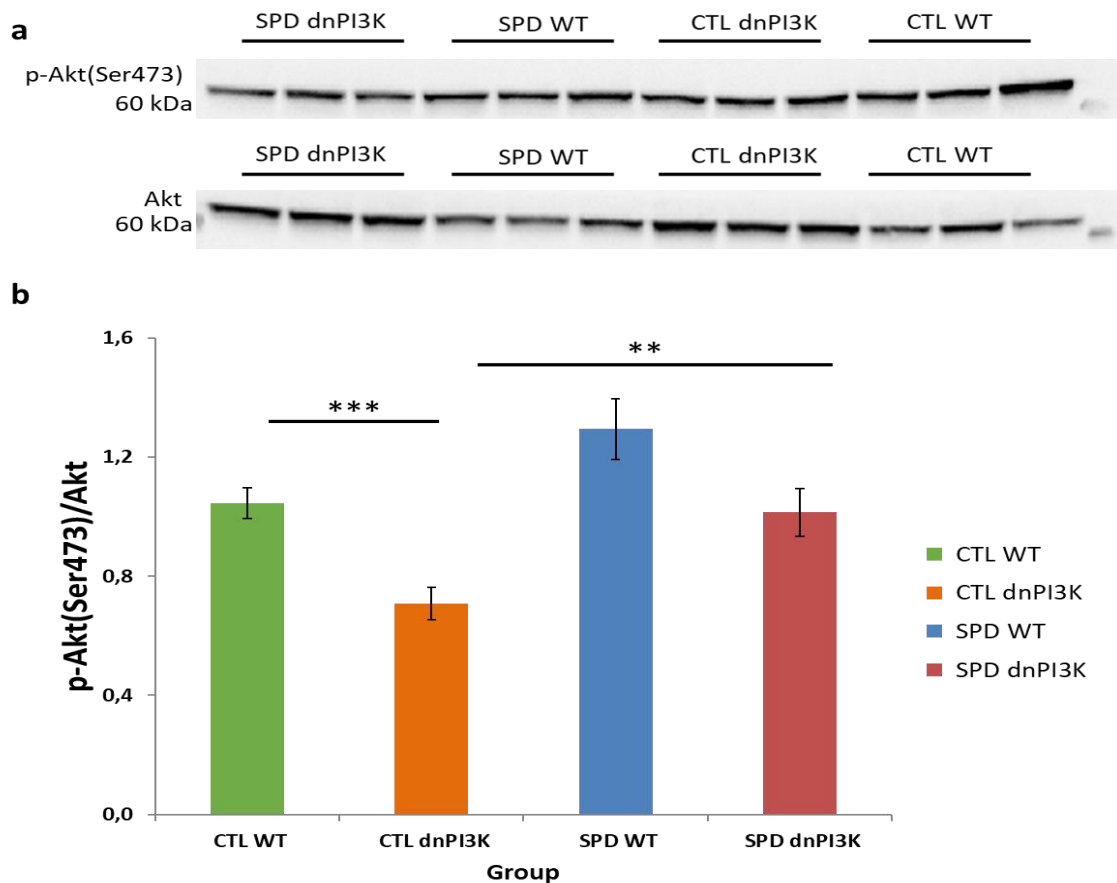
Figure 22: Spermidine increased Akt phosphorylation of Ser473 site in dnPI3K mice. a) Representative Western Blots show (p-Akt(Ser473) (60 kDa) and total Akt (60 kDa). Spermidine-treated groups were subjected to i.p. injections of spermidine (50 mg/kg body weight SPD in 0.9% NaCl), whereas control groups received injections of 0.9% NaCl **b)** Blots were quantified by densitometry and normalized to the loading control. N=8 mice/group. ***$p<0.0001$, **$p<0.01$. Abbreviations: m - months, SPD – spermidine, CTL - control

To further elucidate mechanisms underlying the IGF-1/PI3K signaling pathway, Western Blotting was performed on the Akt downstream target mTOR.

3.8   mTOR expression in dnPI3K mice

There were no significant differences in the mTOR expression in any of the groups tested at baseline and after spermidine treatment (Figure 23). However, our statistical analysis revealed that spermidine reduced mTOR expression as a main.
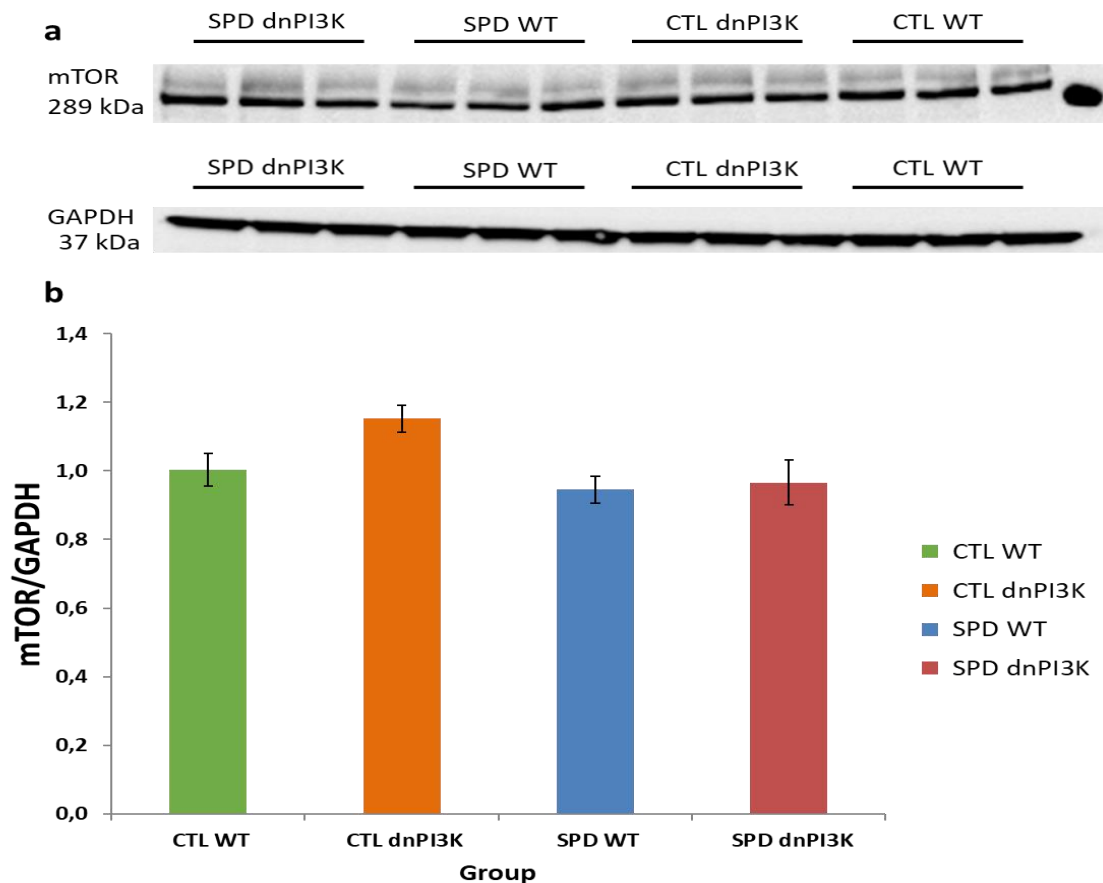
Figure 23: Expression of mTOR in dnPI3K mice. a) Representative Western Blots show mTOR (289 kDa) and GAPDH (37 kDa) as a loading control. **b)** Blots were quantified by densitometry and normalized to the loading control. N=8 mice/group. Abbreviations: m - months, SPD – spermidine, CTL - control

3.9 Phosphorylation of FoxO3a in dnPI3K mice

Another important downstream effector of the IGF-1/PI3K pathway is FoxO transcription factors family. Therefore, we investigated the activity of FoxO3a transcription factor in the IGF-1/PI3K/Akt signaling, as FoxO3a is an important determinant of autophagy induction [63]. The activity of FoxO3a is regulated by Akt and its phosphorylation leads to inactivation of FoxO3a.

dnPI3K mice had reduced phosphorylation of FoxO3a (P=0,045; Figure 24) than WT animals under control conditions. Interestingly, both groups responded differently to the treatment with spermidine, which significantly reduced FoxO3a phosphorylation in WT hearts (P= 0,039), while tended to increase FoxO3a phosphorylation in dnPI3K mice (Figure 24).
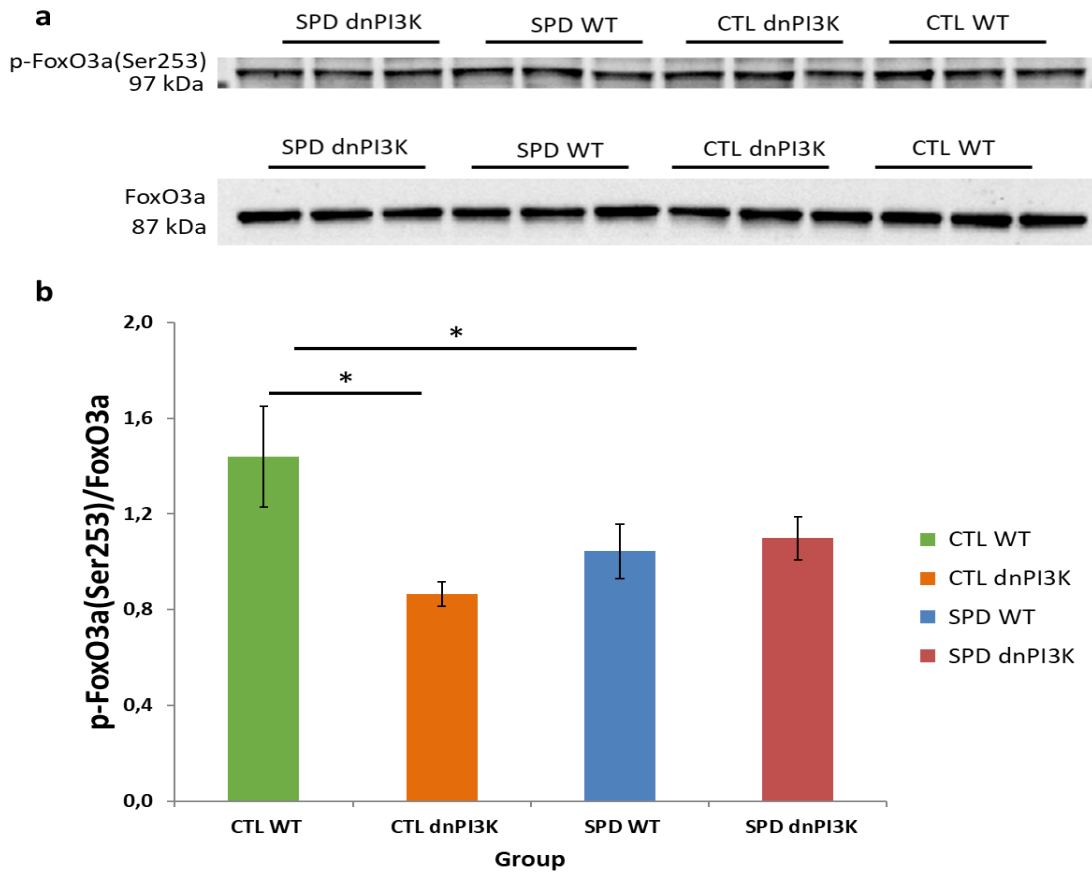
Figure 24: Expression of p-FoxO3a in dnPI3K mice. a) Original Western Blots showing p-FoxO3a(Ser253) (97 kDa) and total expression of FoxO3a (87 kDa). Treated groups (SPD) were subjected to i.p. injections of spermidine (50 mg/kg body weight SPD in 0.9% NaCl), whereas the control groups received injections of 0.9% NaCl **b)** Blots were quantified by densitometry and normalized to the loading control. N=8 mice/group. *P<0.05. Abbreviations: m - months, SPD – spermidine, CTL - control

An overview of the observed effects of spermidine on the IGF-1/PI3K signaling pathway is shown in Table 4.

Table 4 Effects of spermidine on the IGF-1/PI3K signaling pathway in the mouse heart

Mouse model	IGF-1R/PI3K downstream target	Effect (control animals)	Effect (spermidine treatment)
IGF-1R	IGF-1	increased	reduced
IGF-1R	Akt	reduced	no change
IGF-1R	p-Akt(Thr308)	increased	No change
IGF-1R	p-Akt(Thr308)	increased	reduced (after i.p. injections)
IGF-1R	p-Akt(Ser473)	increased	reduced
IGF-1R	mTOR	no effect	no change
dnPI3K	Akt	increased	no change
dnPI3K	p-Akt(Thr308)	reduced	reduced
dnPI3K	p-Akt(Ser473)	reduced	increased
dnPI3K	mTOR	no effect	no change
dnPI3K	p-FoxO3a	reduced	increased

4 Discussion

The aim of the present study was to examine the role of spermidine on the IGF-1/PI3K signaling pathway in the mouse heart and to elucidate its downstream signaling targets as well as transcriptional regulatory effects. To this end, we used young and middle-aged mice overexpressing cardiomyocyte-specific IGF-1 and mice, harbouring cardiomyocyte-specific inhibition of PI3K (dnPI3K). Given that IGF-1 is implicated as a primary factor in the development of cardiac hypertrophy [119], it is relevant to define pharmacological strategies that regulate the IGF-1/PI3K pathway, and thus to prevent age-associated hypertrophy coupled to cardiac aging. The role of IGF-1 signaling in the heart has been determined using genetic animal models with overexpression [36] or deletion [43, 43] of the IGF-1R in the heart. The main advantage of such models is that they allow to define the role of the IGF-1 signaling cascade specifically in the heart.

Our results show that oral supplementation of spermidine reduced the expression of IGF-1R in the IGF-1R mice, but not in WT animals, suggesting that spermidine appears more effective to delay cardiac aging, when there is an excessive expression of the IGF-1 receptor, reasons that may account for this effect remain elusive, but could include epigenetic mechanisms underlying reduced transcription of genes due to high deacetylation capacity by spermidine [120].

Studies demonstrated the beneficial effects of reduced IGF-1 signaling on cardiac aging [43, 44]. For example, a recent study by Ock *et al.* showed that aging was associated with the induction of IGF-1R expression in cardiomyocytes. Furthermore, the same authors showed that hypertrophic response associated with aging was blunted and cardiac function was preserved in cardiomyocyte-specific IGF-1R knockout mice [43]. Consistent with this, transgenic mice overexpressing the IGF-1R in the heart (used in this study) display cardiac hypertrophy, yet without any evidence of histopathology [36], which may occur later in life.

To find out whether spermidine supplementation negatively regulates the IGF-1 signaling cascade, we performed immunoblot analysis on heart lysates from IGF-1R mice and dnPI3K mice. Akt (Protein kinase B) is one of the best known downstream signaling targets of the IGF-1/PI3K cascade. IGF-1 stimulates the PI3K/Akt pathway via PI3K, which is activated by its interaction with the insulin receptor substrate (IRS) to the activation of Akt. Akt is translocated from the cytoplasm to the cell membrane, where it is phosphorylated at Thr308 and Ser473 sites and phosphorylation of both residues is required to generate a high level of Akt activity [53]. We could show that hyperactivation of the IGF-1/PI3K pathway led to a significant reduction of Akt expression in the IGF-1R hearts. This is corroborated by an increased expression of Akt

in mice with dominant negative PI3K. Our findings indicate that there is a compensatory mechanism, which prevents from an excessive expression of Akt likely due to high expression levels of IGF-1R. We also found an elevated phosphorylation of Thr308 and Ser473 residue in IGF-1R hearts. In conjunction with reduced Akt expression, increased phosphorylation of Akt indicates increased Akt activity in IGF-1R mice. In contrast, aged cardiomyocyte-specific IGF-1R knockout mice show lower levels of Akt phosphorylation compared to aged WT littermates [43]. A recent study showed that a cardiac-specific Akt overexpression contributes to chronic activation of Akt and therefore accentuates an aging-induced decline in autophagy [34], suggesting that an increase in Akt phosphorylation with aging may be responsible for reduced autophagic activity and age-associated complications. These data imply that Akt activation is responsible for the inhibition of autophagy in aging, and thus promotes cardiac dysfunction associated with aging.

While chronic spermidine changed neither Akt expression nor the phosphorylation of Thr308 site in IGF-1R and WT hearts, we observed a strong trend toward reduced phosphorylation at Ser473 site upon long-term spermidine treatment only in WT mice. Interestingly, a similar effect on Thr308 phosphorylation was found in IGF-1R mice, that received intraperitoneal. injections of spermidine (i.e. acute treatment). Izumo *et al.* showed that the amount of phosphorylated Akt is increased in constitutively active PI3K mice, whereas the amount of non-phosphorylated Akt is expectedly decreased. Conversely, levels of phosphorylated Akt in dnPI3K mice are decreased and the amount of the non-phosphorylated form of Akt was elevated [49]. Consistent with these results, our dnPI3K mice showed decreased phosphorylation of Akt and thus reduced Akt activity. In addition, acute administration of spermidine caused about 2-fold reduction of Thr308 phosphorylation in WT mice, while exerting no effect in dnPI3K mice. In contrast, administration of spermidine increased the phosphorylation of Ser473 site in WT mice and also dnPI3K animals. Altogether, these results indicate that spermidine negatively and positively regulates these two Akt phosphorylation sites (i.e. Thr308, Ser473, respectively), suggesting likely different mechanisms, which need to be further explored in future studies. Consistent with our results, Chrisam *et al.* reported that chronic spermidine administration decreases Akt phosphorylation levels in skeletal muscle [105].

We observed that spermidine supplementation reduced the phosphorylation/activation of Akt in WT mice, but not in IGF-1R and dnPI3K mice, indicating that spermidine has limited capacity to counteract the alterations caused by the mutations. Our results also show that different route (oral vs. intraperitoneal) and treatment duration (acute vs. chronic) of spermidine have slightly different effects on the IGF-1/PI3K signaling pathway, albeit we have to point out

that different mouse models were used due to their availability at the time of experiments. Therefore, it would be highly informative to perform acute and chronic treatment in both transgenic models (e.g. IGF-1R and dnPI3K).

FoxO transcription factors have been implicated in the regulation of several cellular functions, including the induction of autophagy [63]. FoxO3a is subjected to inhibition by IGF-1 and overexpression of IGF-1R induces FoxO3a phosphorylation, which is triggered by PI3K/Akt pathway [121]. On the one hand, phosphorylated FoxO3a proteins are inactive and are sequestered in the cytoplasm where they are unable to regulate gene expression. On the other hand, dephosphorylated FoxO3a transcription factors are activated and translocated to the nucleus, where they activate the transcription of autophagy-related genes. Our results show a significant decrease of FoxO3a phosphorylation in dnPI3K mice, indicating that decreased activity of the IGF-1/PI3K/Akt signaling pathway due to the mutation is responsible for the dephosphorylation of FoxO3a, and thus activation of FoxO3a transcription factor. Our study confirms findings from previous studies, which demonstrated that FoxO transcription factors are inactivated via the IGF-1/PI3K/Akt pathway [60, 63, 121]. Importantly, spermidine reduced phosphorylation of FoxO3a in WT mice, indicating that spermidine is able to induce FoxO activity, which might be associated with increased autophagy [63]. We detected a decrease of mTOR expression upon spermidine treatment in WT as well as in dnPI3K as a main effect, while we could not observe any changes in mTOR expression levels in IGF-1R and dnPI3K mice under control conditions. Based on our finding that spermidine promotes dephosphorylation of Akt and FoxO3a, it is tempting to speculate that spermidine triggers translocation of FoxO3a into the nucleus, causing increased transcription of autophagy-related genes. Additional experiments are warranted to determine whether autophagic flux is reduced in our IGF-1R overexpressing mice, and whether spermidine activates autophagy in these mice.

In this work we have demonstrated that oral spermidine supplementation or intraperitoneal injections of spermidine inhibit, at least in part, the IGF-1/PI3K signaling pathway in the heart. Reduced phosphorylation of Akt at site Thr308 as well as dephosphorylation of FoxO3a seems to be important downstream targets of the IGF-1/PI3K pathway underlying cardioprotective effects by spermidine. Further investigation is needed to elucidate the precise role of spermidine in this complex molecular pathway of aging and longevity.

5   References

[1] Christensen, K.; Doblhammer, G.; Rau, R.; Vaupel, J.W. Ageing populations: The challenges ahead. *The Lancet*, **2009**, *374,* 1196–1208.

[2] Kontis, V.; Bennett, J.E.; Mathers, C.D.; Li, G.; Foreman, K.; Ezzati, M. Future life expectancy in 35 industrialised countries: Projections with a Bayesian model ensemble. *The Lancet*, **2017**, *389,* 1323–1335.

[3] Chatterji, S.; Byles, J.; Cutler, D.; Seeman, T.; Verdes, E. Health, functioning, and disability in older adults—present status and future implications. *The Lancet*, **2015**, *385,* 563–575.

[4] Guzman-Castillo, M.; Ahmadi-Abhari, S.; Bandosz, P.; Capewell, S.; Steptoe, A.; Singh-Manoux, A.; Kivimaki, M.; Shipley, M.J.; Brunner, E.J.; O'Flaherty, M. Forecasted trends in disability and life expectancy in England and Wales up to 2025: A modelling study. *The Lancet Public Health*, **2017**, *2,* e307-e313.

[5] Lakatta, E.G. Arterial and Cardiac Aging: Major Shareholders in Cardiovascular Disease Enterprises: Part I: Aging Arteries: A "Set Up" for Vascular Disease. *Circulation*, **2003**, *107,* 139–146.

[6] North, B.J.; Sinclair, D.A. The intersection between aging and cardiovascular disease. *Circulation research*, **2012**, *110,* 1097–1108.

[7] Fontana, L.; Partridge, L.; Longo, V.D. Extending healthy life span--from yeast to humans. *Science (New York, N.Y.)*, **2010**, *328,* 321–326.

[8] Saetrum Opgaard, O.; Wang, P.H. IGF-I is a matter of heart. *Growth hormone & IGF research : official journal of the Growth Hormone Research Society and the International IGF Research Society*, **2005**, *15,* 89–94.

[9] Rincon, M.; Rudin, E.; Barzilai, N. The insulin/IGF-1 signaling in mammals and its relevance to human longevity. *Experimental gerontology*, **2005**, *40,* 873–877.

[10] Berryman, D.E.; Christiansen, J.S.; Johannsson, G.; Thorner, M.O.; Kopchick, J.J. Role of the GH/IGF-1 axis in lifespan and healthspan: Lessons from animal models. *Growth hormone & IGF research : official journal of the Growth Hormone Research Society and the International IGF Research Society*, **2008**, *18,* 455–471.

[11] Bergmann, O.; Bhardwaj, R.D.; Bernard, S.; Zdunek, S.; Barnabé-Heider, F.; Walsh, S.; Zupicich, J.; Alkass, K.; Buchholz, B.A.; Druid, H.; Jovinge, S.; Frisén, J. Evidence for cardiomyocyte renewal in humans. *Science (New York, N.Y.)*, **2009**, *324,* 98–102.

[12] Anversa, P.; Sonnenblick, E.H. Ischemic cardiomyopathy: Pathophysiologic mechanisms. *Progress in cardiovascular diseases*, **1990**, *33,* 49–70.

[13] Wei, J.Y. Age and the cardiovascular system. *The New England journal of medicine*, **1992**, *327,* 1735–1739.

[14] Goldspink, D.F.; Burniston, J.G.; Tan, L.-B. Cardiomyocyte death and the ageing and failing heart. *Experimental physiology*, **2003**, *88,* 447–458.

[15] Olivetti, G.; Melissari, M.; Capasso, J.M.; Anversa, P. Cardiomyopathy of the aging human heart. Myocyte loss and reactive cellular hypertrophy. *Circulation research*, **1991**, *68,* 1560–1568.

[16] Bernhard, D.; Laufer, G. The aging cardiomyocyte: A mini-review. *Gerontology*, **2008**, *54,* 24–31.

[17] Lavandero, S.; Chiong, M.; Rothermel, B.A.; Hill, J.A. Autophagy in cardiovascular biology. *The Journal of clinical investigation*, **2015**, *125,* 55–64.

[18] Maillet, M.; van Berlo, J.H.; Molkentin, J.D. Molecular basis of physiological heart growth: Fundamental concepts and new players. *Nature reviews. Molecular cell biology*, **2013**, *14,* 38–48.

[19] Krenning, G.; Zeisberg, E.M.; Kalluri, R. The origin of fibroblasts and mechanism of cardiac fibrosis. *Journal of cellular physiology*, **2010**, *225,* 631–637.

[20] Strait, J.B.; Lakatta, E.G. Aging-associated cardiovascular changes and their relationship to heart failure. *Heart failure clinics*, **2012**, *8,* 143–164.

[21] Herraiz-Martínez, A.; Álvarez-García, J.; Llach, A.; Molina, C.E.; Fernandes, J.; Ferrero-Gregori, A.; Rodríguez, C.; Vallmitjana, A.; Benítez, R.; Padró, J.M.; Martínez-González, J.; Cinca, J.; Hove-Madsen, L. Ageing is associated with deterioration of calcium homeostasis in isolated human right atrial myocytes. *Cardiovascular research*, **2015**, *106,* 76–86.

[22] Terman, A.; Brunk, U.T. Myocyte aging and mitochondrial turnover. *Experimental gerontology*, **2004**, *39,* 701–705.

[23] Dai, D.-F.; Rabinovitch, P.S.; Ungvari, Z. Mitochondria and cardiovascular aging. *Circulation research*, **2012**, *110,* 1109–1124.

[24] Dutta, D.; Calvani, R.; Bernabei, R.; Leeuwenburgh, C.; Marzetti, E. Contribution of impaired mitochondrial autophagy to cardiac aging: Mechanisms and therapeutic opportunities. *Circulation research*, **2012**, *110,* 1125–1138.

[25] Tocchi, A.; Quarles, E.K.; Basisty, N.; Gitari, L.; Rabinovitch, P.S. Mitochondrial dysfunction in cardiac aging. *Biochimica et biophysica acta*, **2015**, *1847,* 1424–1433.

[26] Johnson, S.C.; Rabinovitch, P.S.; Kaeberlein, M. mTOR is a key modulator of ageing and age-related disease. *Nature*, **2013**, *493,* 338–345.

[27] Luong, N.; Davies, C.R.; Wessells, R.J.; Graham, S.M.; King, M.T.; Veech, R.; Bodmer, R.; Oldham, S.M. Activated FOXO-mediated insulin resistance is blocked by reduction of TOR activity. *Cell metabolism*, **2006**, *4,* 133–142.

[28] Meikle, L.; McMullen, J.R.; Sherwood, M.C.; Lader, A.S.; Walker, V.; Chan, J.A.; Kwiatkowski, D.J. A mouse model of cardiac rhabdomyoma generated by loss of Tsc1 in ventricular myocytes. *Human molecular genetics*, **2005**, *14,* 429–435.

[29] Laplante, M.; Sabatini, D.M. mTOR signaling in growth control and disease. *Cell*, **2012**, *149,* 274–293.

[30] Vézina, C.; Kudelski, A.; Sehgal, S.N. Rapamycin (AY-22,989), a new antifungal antibiotic. I. Taxonomy of the producing streptomycete and isolation of the active principle. *The Journal of antibiotics*, **1975**, *28,* 721–726.

[31] McMullen, J.R.; Sherwood, M.C.; Tarnavski, O.; Zhang, L.; Dorfman, A.L.; Shioi, T.; Izumo, S. Inhibition of mTOR signaling with rapamycin regresses established cardiac hypertrophy induced by pressure overload. *Circulation*, **2004**, *109,* 3050–3055.

[32] Paddenberg, R.; Stieger, P.; Lilien, A.-L. von; Faulhammer, P.; Goldenberg, A.; Tillmanns, H.H.; Kummer, W.; Braun-Dullaeus, R.C. Rapamycin attenuates hypoxia-induced pulmonary vascular remodeling and right ventricular hypertrophy in mice. *Respiratory research*, **2007**, *8,* 15.

[33] Gao, X.-M.; Wong, G.; Wang, B.; Kiriazis, H.; Moore, X.-L.; Su, Y.-D.; Dart, A.; Du, X.-J. Inhibition of mTOR reduces chronic pressure-overload cardiac hypertrophy and fibrosis. *Journal of hypertension*, **2006**, *24,* 1663–1670.

[34] Hua, Y.; Zhang, Y.; Ceylan-Isik, A.F.; Wold, L.E.; Nunn, J.M.; Ren, J. Chronic Akt activation accentuates aging-induced cardiac hypertrophy and myocardial contractile dysfunction: Role of autophagy. *Basic research in cardiology*, **2011**, *106,* 1173–1191.

[35] Dai, D.-F.; Chen, T.; Johnson, S.C.; Szeto, H.; Rabinovitch, P.S. Cardiac aging: From molecular mechanisms to significance in human health and disease. *Antioxidants & redox signaling*, **2012**, *16,* 1492–1526.

[36] McMullen, J.R.; Shioi, T.; Huang, W.-Y.; Zhang, L.; Tarnavski, O.; Bisping, E.; Schinke, M.; Kong, S.; Sherwood, M.C.; Brown, J.; Riggi, L.; Kang, P.M.; Izumo, S. The insulin-like growth factor 1 receptor induces physiological heart growth via the phosphoinositide 3-kinase(p110alpha) pathway. *The Journal of biological chemistry*, **2004**, *279,* 4782–4793.

[37] Kaplan, R.C.; Strickler, H.D.; Rohan, T.E.; Muzumdar, R.; Brown, D.L. Insulin-like growth factors and coronary heart disease. *Cardiology in review*, **2005**, *13,* 35–39.

[38] Troncoso, R.; Ibarra, C.; Vicencio, J.M.; Jaimovich, E.; Lavandero, S. New insights into IGF-1 signaling in the heart. *Trends in endocrinology and metabolism: TEM*, **2014**, *25,* 128–137.

[39] Suleiman, M.-S.; Singh, R.J.R.; Stewart, C.E.H. Apoptosis and the cardiac action of insulin-like growth factor I. *Pharmacology & therapeutics*, **2007**, *114,* 278–294.

[40] McMullen, J.R. Role of insulin-like growth factor 1 and phosphoinositide 3-kinase in a setting of heart disease. *Clinical and experimental pharmacology & physiology*, **2008**, *35,* 349–354.

[41] Reiss, K.; Cheng, W.; Ferber, A.; Kajstura, J.; Li, P.; Li, B.; Olivetti, G.; Homcy, C.J.; Baserga, R.; Anversa, P. Overexpression of insulin-like growth factor-1 in the heart is coupled with myocyte proliferation in transgenic mice. *Proceedings of the National Academy of Sciences of the United States of America*, **1996,** *93,* 8630–8635.

[42] Ren, J.; Samson, W.K.; Sowers, J.R. Insulin-like growth factor I as a cardiac hormone: Physiological and pathophysiological implications in heart disease. *Journal of molecular and cellular cardiology*, **1999**, *31,* 2049–2061.

[43] Ock, S.; Lee, W.S.; Ahn, J.; Kim, H.M.; Kang, H.; Kim, H.-S.; Jo, D.; Abel, E.D.; Lee, T.J.; Kim, J. Deletion of IGF-1 Receptors in Cardiomyocytes Attenuates Cardiac Aging in Male Mice. *Endocrinology*, **2016**, *157,* 336–345.

[44] Wessells, R.J.; Fitzgerald, E.; Cypser, J.R.; Tatar, M.; Bodmer, R. Insulin regulation of heart function in aging fruit flies. *Nature genetics*, **2004**, *36,* 1275–1281.

[45] Delaughter, M.C.; Taffet, G.E.; Fiorotto, M.L.; Entman, M.L.; Schwartz, R.J. Local insulin-like growth factor I expression induces physiologic, then pathologic, cardiac hypertrophy in transgenic mice. *The FASEB Journal*, **1999**, *13,* 1923–1929.

[46] Corpas, E.; Harman, S.M.; Blackman, M.R. Human growth hormone and human aging. *Endocrine reviews*, **1993**, *14,* 20–39.

[47] Vasan, R.S.; Sullivan, L.M.; D'Agostino, R.B.; Roubenoff, R.; Harris, T.; Sawyer, D.B.; Levy, D.; Wilson, P.W.F. Serum insulin-like growth factor I and risk for heart failure in elderly individuals without a previous myocardial infarction: The Framingham Heart Study. *Annals of internal medicine*, **2003**, *139,* 642–648.

[48] Luo, J.; McMullen, J.R.; Sobkiw, C.L.; Zhang, L.; Dorfman, A.L.; Sherwood, M.C.; Logsdon, M.N.; Horner, J.W.; DePinho, R.A.; Izumo, S.; Cantley, L.C. Class IA phosphoinositide 3-kinase regulates heart size and physiological cardiac hypertrophy. *Molecular and cellular biology*, **2005**, *25,* 9491–9502.

[49] Shioi, T.; Kang, P.M.; Douglas, P.S.; Hampe, J.; Yballe, C.M.; Lawitts, J.; Cantley, L.C.; Izumo, S. The conserved phosphoinositide 3-kinase pathway determines heart size in mice. *The EMBO journal*, **2000**, *19,* 2537–2548.

[50] DeBosch, B.; Treskov, I.; Lupu, T.S.; Weinheimer, C.; Kovacs, A.; Courtois, M.; Muslin, A.J. Akt1 is required for physiological cardiac growth. *Circulation*, **2006**, *113,* 2097–2104.

[51] Schiaffino, S.; Mammucari, C. Regulation of skeletal muscle growth by the IGF1-Akt/PKB pathway: Insights from genetic models. *Skeletal muscle*, **2011**, *1,* 4.

[52] Toker, A.; Newton, A.C. Akt/protein kinase B is regulated by autophosphorylation at the hypothetical PDK-2 site. *The Journal of biological chemistry*, **2000**, *275,* 8271–8274.

[53] Sarbassov, D.D.; Guertin, D.A.; Ali, S.M.; Sabatini, D.M. Phosphorylation and regulation of Akt/PKB by the rictor-mTOR complex. *Science (New York, N.Y.)*, **2005**, *307,* 1098–1101.

[54] Shioi, T.; McMullen, J.R.; Kang, P.M.; Douglas, P.S.; Obata, T.; Franke, T.F.; Cantley, L.C.; Izumo, S. Akt/protein kinase B promotes organ growth in transgenic mice. *Molecular and cellular biology*, **2002**, *22,* 2799–2809.

[55] Huang, H.; Tindall, D.J. Dynamic FoxO transcription factors. *Journal of cell science*, **2007**, *120,* 2479–2487.

[56] Evans-Anderson, H.J.; Alfieri, C.M.; Yutzey, K.E. Regulation of cardiomyocyte proliferation and myocardial growth during development by FOXO transcription factors. *Circulation research*, **2008**, *102, 686–694.

[57] Hay, N. Interplay between FOXO, TOR, and Akt. *Biochimica et biophysica acta*, **2011**, *1813,* 1965–1970.

[58] Tzivion, G.; Dobson, M.; Ramakrishnan, G. FoxO transcription factors; Regulation by AKT and 14-3-3 proteins. *Biochimica et biophysica acta*, **2011**, *1813,* 1938–1945.

[59] Hosaka, T.; Biggs, W.H.; Tieu, D.; Boyer, A.D.; Varki, N.M.; Cavenee, W.K.; Arden, K.C. Disruption of forkhead transcription factor (FOXO) family members in mice reveals their functional diversification. *Proceedings of the National Academy of Sciences of the United States of America*, **2004**, *101,* 2975–2980.

[60] Ni, Y.G.; Berenji, K.; Wang, N.; Oh, M.; Sachan, N.; Dey, A.; Cheng, J.; Lu, G.; Morris, D.J.; Castrillon, D.H.; Gerard, R.D.; Rothermel, B.A.; Hill, J.A. Foxo transcription factors blunt cardiac hypertrophy by inhibiting calcineurin signaling. *Circulation*, **2006**, *114,* 1159–1168.

[61] Zhao, J.; Brault, J.J.; Schild, A.; Cao, P.; Sandri, M.; Schiaffino, S.; Lecker, S.H.; Goldberg, A.L. FoxO3 coordinately activates protein degradation by the autophagic/lysosomal and proteasomal pathways in atrophying muscle cells. *Cell metabolism*, **2007**, *6,* 472–483.

[62] Ronnebaum, S.M.; Patterson, C. The FoxO family in cardiac function and dysfunction. *Annual review of physiology*, **2010**, *72,* 81–94.

[63] Sengupta, A.; Molkentin, J.D.; Yutzey, K.E. FoxO transcription factors promote autophagy in cardiomyocytes. *The Journal of biological chemistry*, **2009**, *284,* 28319–28331.

[64] Martinou, J.-C.; Kroemer, G. Autophagy: Evolutionary and pathophysiological insights. *Biochimica et biophysica acta*, **2009**, *1793,* 1395–1396.

[65] Galluzzi, L.; Pietrocola, F.; Levine, B.; Kroemer, G. Metabolic control of autophagy. *Cell*, **2014**, *159,* 1263–1276.

[66] Mizushima, N.; Komatsu, M. Autophagy: Renovation of cells and tissues. *Cell*, **2011**, *147,* 728–741.

[67] van Beek, N.; Klionsky, D.J.; Reggiori, F. Genetic aberrations in macroautophagy genes leading to diseases. *Biochimica et biophysica acta*, **2018**, *1865,* 803–816.

[68] Ohsumi, Y. Historical landmarks of autophagy research. *Cell research*, **2014**, *24,* 9–23.

[69] Wesselborg, S.; Stork, B. Autophagy signal transduction by ATG proteins: From hierarchies to networks. *Cellular and molecular life sciences : CMLS*, **2015**, *72,* 4721–4757.

[70] Klionsky, D.J. Autophagy: From phenomenology to molecular understanding in less than a decade. *Nature reviews. Molecular cell biology*, **2007**, *8,* 931–937.

[71] Cuervo, A.M.; Wong, E. Chaperone-mediated autophagy: Roles in disease and aging. *Cell research*, **2014**, *24,* 92–104.

[72] Kaur, J.; Debnath, J. Autophagy at the crossroads of catabolism and anabolism. *Nature reviews. Molecular cell biology*, **2015**, *16,* 461–472.

[73] Farré, J.-C.; Subramani, S. Mechanistic insights into selective autophagy pathways: Lessons from yeast. *Nature reviews. Molecular cell biology*, **2016**, *17,* 537–552.

[74] Bravo-San Pedro, J.M.; Kroemer, G.; Galluzzi, L. Autophagy and Mitophagy in Cardiovascular Disease. *Circulation research*, **2017**, *120,* 1812–1824.

[75] Li, Z.; Wang, J.; Yang, X. Functions of autophagy in pathological cardiac hypertrophy. *International journal of biological sciences*, **2015**, *11,* 672–678.

[76] Laplante, M.; Sabatini, D.M. Regulation of mTORC1 and its impact on gene expression at a glance. *Journal of cell science*, **2013**, *126,* 1713–1719.

[77] Kamada, Y.; Yoshino, K.-i.; Kondo, C.; Kawamata, T.; Oshiro, N.; Yonezawa, K.; Ohsumi, Y. Tor directly controls the Atg1 kinase complex to regulate autophagy. *Molecular and cellular biology*, **2010**, *30,* 1049–1058.

[78] Taneike, M.; Nishida, K.; Omiya, S.; Zarrinpashneh, E.; Misaka, T.; Kitazume-Taneike, R.; Austin, R.; Takaoka, M.; Yamaguchi, O.; Gambello, M.J.; Shah, A.M.; Otsu, K. mTOR Hyperactivation by Ablation of Tuberous Sclerosis Complex 2 in the Mouse Heart Induces Cardiac Dysfunction with the Increased Number of Small Mitochondria Mediated through the Down-Regulation of Autophagy. *PloS one*, **2016**, *11,* e0152628.

[79] Russell, R.C.; Yuan, H.-X.; Guan, K.-L. Autophagy regulation by nutrient signaling. *Cell research*, **2014**, *24,* 42–57.

[80] Kim, J.; Kundu, M.; Viollet, B.; Guan, K.-L. AMPK and mTOR regulate autophagy through direct phosphorylation of Ulk1. *Nature cell biology*, **2011**, *13,* 132–141.

[81] Turdi, S.; Fan, X.; Li, J.; Zhao, J.; Huff, A.F.; Du, M.; Ren, J. AMP-activated protein kinase deficiency exacerbates aging-induced myocardial contractile dysfunction. *Aging cell*, **2010**, *9,* 592–606.

[82] Egan, D.F.; Shackelford, D.B.; Mihaylova, M.M.; Gelino, S.; Kohnz, R.A.; Mair, W.; Vasquez, D.S.; Joshi, A.; Gwinn, D.M.; Taylor, R.; Asara, J.M.; Fitzpatrick, J.; Dillin, A.; Viollet, B.; Kundu, M.; Hansen, M.; Shaw, R.J. Phosphorylation of ULK1 (hATG1) by AMP-activated protein kinase connects energy sensing to mitophagy. *Science (New York, N.Y.)*, **2011**, *331,* 456–461.

[83] Sandri, M.; Sandri, C.; Gilbert, A.; Skurk, C.; Calabria, E.; Picard, A.; Walsh, K.; Schiaffino, S.; Lecker, S.H.; Goldberg, A.L. Foxo transcription factors induce the atrophy-related ubiquitin ligase atrogin-1 and cause skeletal muscle atrophy. *Cell*, **2004**, *117,* 399–412.

[84] Brunet, A.; Sweeney, L.B.; Sturgill, J.F.; Chua, K.F.; Greer, P.L.; Lin, Y.; Tran, H.; Ross, S.E.; Mostoslavsky, R.; Cohen, H.Y.; Hu, L.S.; Cheng, H.-L.; Jedrychowski, M.P.; Gygi, S.P.; Sinclair, D.A.; Alt, F.W.; Greenberg, M.E. Stress-dependent regulation of FOXO transcription factors by the SIRT1 deacetylase. *Science (New York, N.Y.)*, **2004**, *303,* 2011–2015.

[85] Lee, I.H.; Cao, L.; Mostoslavsky, R.; Lombard, D.B.; Liu, J.; Bruns, N.E.; Tsokos, M.; Alt, F.W.; Finkel, T. A role for the NAD-dependent deacetylase Sirt1 in the regulation of autophagy. *Proceedings of the National Academy of Sciences of the United States of America*, **2008**, *105,* 3374–3379.

[86] Cohen, E.; Paulsson, J.F.; Blinder, P.; Burstyn-Cohen, T.; Du, D.; Estepa, G.; Adame, A.; Pham, H.M.; Holzenberger, M.; Kelly, J.W.; Masliah, E.; Dillin, A. Reduced IGF-1 signaling delays age-associated proteotoxicity in mice. *Cell*, **2009**, *139,* 1157–1169.

[87] Holzenberger, M.; Dupont, J.; Ducos, B.; Leneuve, P.; Géloën, A.; Even, P.C.; Cervera, P.; Le Bouc, Y. IGF-1 receptor regulates lifespan and resistance to oxidative stress in mice. *Nature*, **2003**, *421,* 182–187.

[88] Bitto, A.; Lerner, C.; Torres, C.; Roell, M.; Malaguti, M.; Perez, V.; Lorenzini, A.; Hrelia, S.; Ikeno, Y.; Matzko, M.E.; McCarter, R.; Sell, C. Long-term IGF-I exposure decreases autophagy and cell viability. *PloS one*, **2010**, *5,* e12592.

[89] Troncoso, R.; Vicencio, J.M.; Parra, V.; Nemchenko, A.; Kawashima, Y.; Del Campo, A.; Toro, B.; Battiprolu, P.K.; Aranguiz, P.; Chiong, M.; Yakar, S.; Gillette, T.G.; Hill, J.A.; Abel, E.D.; Leroith, D.; Lavandero, S. Energy-preserving effects of IGF-1 antagonize starvation-induced cardiac autophagy. *Cardiovascular research*, **2012**, *93,* 320–329.

[90] Matsui, Y.; Takagi, H.; Qu, X.; Abdellatif, M.; Sakoda, H.; Asano, T.; Levine, B.; Sadoshima, J. Distinct roles of autophagy in the heart during ischemia and reperfusion: Roles of AMP-activated protein kinase and Beclin 1 in mediating autophagy. *Circulation research*, **2007**, *100,* 914–922.

[91] Troncoso, R.; Díaz-Elizondo, J.; Espinoza, S.P.; Navarro-Marquez, M.F.; Oyarzún, A.P.; Riquelme, J.A.; Garcia-Carvajal, I.; Díaz-Araya, G.; García, L.; Hill, J.A.; Lavandero, S. Regulation of cardiac autophagy by insulin-like growth factor 1. *IUBMB life*, **2013**, *65,* 593–601.

[92] Swynghedauw, B.; Besse, S.; Assayag, P.; Carré, F.; Chevalier, B.; Charlemagne, D.; Delcayre, C.; Hardouin, S.; Heymes, C.; Moalic, J.M. Molecular and cellular biology of the senescent hypertrophied and failing heart. *The American journal of cardiology*, **1995**, *76,* 2D-7D.

[93] Stadtman, E.R. Protein oxidation in aging and age-related diseases. *Annals of the New York Academy of Sciences*, **2001**, *928,* 22–38.

[94] Shirakabe, A.; Ikeda, Y.; Sciarretta, S.; Zablocki, D.K.; Sadoshima, J. Aging and Autophagy in the Heart. *Circulation research*, **2016**, *118,* 1563–1576.

[95] Taneike, M.; Yamaguchi, O.; Nakai, A.; Hikoso, S.; Takeda, T.; Mizote, I.; Oka, T.; Tamai, T.; Oyabu, J.; Murakawa, T.; Nishida, K.; Shimizu, T.; Hori, M.; Komuro, I.; Takuji Shirasawa, T.S.; Mizushima, N.; Otsu, K. Inhibition of autophagy in the heart induces age-related cardiomyopathy. *Autophagy*, **2010**, *6,* 600–606.

[96] Tanaka, Y.; Guhde, G.; Suter, A.; Eskelinen, E.L.; Hartmann, D.; Lüllmann-Rauch, R.; Janssen, P.M.; Blanz, J.; Figura, K. von; Saftig, P. Accumulation of autophagic vacuoles and cardiomyopathy in LAMP-2-deficient mice. *Nature*, **2000**, *406,* 902–906.

[97] Ryter, S.W.; Cloonan, S.M.; Choi, A.M.K. Autophagy: A critical regulator of cellular metabolism and homeostasis. *Molecules and cells*, **2013**, *36,* 7–16.

[98] Shintani, T.; Klionsky, D.J. Autophagy in health and disease: A double-edged sword. *Science (New York, N.Y.)*, **2004**, *306,* 990–995.

[99] Cuervo, A.M. Autophagy and aging: Keeping that old broom working. *Trends in genetics : TIG*, **2008**, *24,* 604–612.

[100] López-Otín, C.; Galluzzi, L.; Freije, J.M.P.; Madeo, F.; Kroemer, G. Metabolic Control of Longevity. *Cell*, **2016**, *166,* 802–821.

[101] Madeo, F.; Pietrocola, F.; Eisenberg, T.; Kroemer, G. Caloric restriction mimetics: Towards a molecular definition. *Nature reviews. Drug discovery*, **2014**, *13,* 727–740.

[102] Das, R.; Kanungo, M.S. Activity and modulation of ornithine decarboxylase and concentrations of polyamines in various tissues of rats as a function of age. *Experimental gerontology*, **1982**, *17,* 95–103.

[103] Nishimura, K.; Shiina, R.; Kashiwagi, K.; Igarashi, K. Decrease in polyamines with aging and their ingestion from food and drink. *Journal of biochemistry*, **2006**, *139,* 81–90.

[104] Soda, K.; Kano, Y.; Nakamura, T.; Kasono, K.; Kawakami, M.; Konishi, F. Spermine, a natural polyamine, suppresses LFA-1 expression on human lymphocyte. *Journal of immunology (Baltimore, Md. : 1950)*, **2005**, *175,* 237–245.

[105] Chrisam, M.; Pirozzi, M.; Castagnaro, S.; Blaauw, B.; Polishchuck, R.; Cecconi, F.; Grumati, P.; Bonaldo, P. Reactivation of autophagy by spermidine ameliorates the myopathic defects of collagen VI-null mice. *Autophagy*, **2015**, *11,* 2142–2152.

[106] Nowotarski, S.L.; Woster, P.M.; Casero, R.A. Polyamines and cancer: Implications for chemotherapy and chemoprevention. *Expert reviews in molecular medicine*, **2013**, *15,* e3.

[107] Eisenberg, T.; Abdellatif, M.; Schroeder, S.; Primessnig, U.; Stekovic, S.; Pendl, T.; Harger, A.; Schipke, J.; Zimmermann, A.; Schmidt, A.; Tong, M.; Ruckenstuhl, C.; Dammbrueck, C.; Gross, A.S.; Herbst, V.; Magnes, C.; Trausinger, G.; Narath, S.; Meinitzer, A.; Hu, Z.; Kirsch, A.; Eller, K.; Carmona-Gutierrez, D.; Büttner, S.; Pietrocola, F.; Knittelfelder, O.; Schrepfer, E.; Rockenfeller, P.; Simonini, C.; Rahn, A.; Horsch, M.; Moreth, K.; Beckers, J.; Fuchs, H.; Gailus-Durner, V.; Neff, F.; Janik, D.; Rathkolb, B.; Rozman, J.; Angelis, M.H. de; Moustafa, T.; Haemmerle, G.; Mayr, M.; Willeit, P.; Frieling-Salewsky, M. von; Pieske, B.; Scorrano, L.; Pieber, T.; Pechlaner, R.; Willeit, J.; Sigrist, S.J.; Linke, W.A.; Mühlfeld, C.; Sadoshima, J.; Dengjel, J.;

Kiechl, S.; Kroemer, G.; Sedej, S.; Madeo, F. Cardioprotection and lifespan extension by the natural polyamine spermidine. *Nature medicine*, **2016**, *22,* 1428–1438.

[108] Minois, N. Molecular basis of the 'anti-aging' effect of spermidine and other natural polyamines - a mini-review. *Gerontology*, **2014**, *60,* 319–326.

[109] Bardócz, S.; Duguid, T.J.; Brown, D.S.; Grant, G.; Pusztai, A.; White, A.; Ralph, A. The importance of dietary polyamines in cell regeneration and growth. *BJN*, **1995**, *73,* 819.

[110] Madeo, F.; Eisenberg, T.; Pietrocola, F.; Kroemer, G. Spermidine in health and disease. *Science (New York, N.Y.)*, **2018**, *359*.

[111] Minois, N.; Carmona-Gutierrez, D.; Madeo, F. Polyamines in aging and disease. *Aging*, **2011**, *3,* 716–732.

[112] Tong, D.; Hill, J.A. Spermidine Promotes Cardioprotective Autophagy. *Circulation research*, **2017**, *120,* 1229–1231.

[113] Eisenberg, T.; Abdellatif, M.; Zimmermann, A.; Schroeder, S.; Pendl, T.; Harger, A.; Stekovic, S.; Schipke, J.; Magnes, C.; Schmidt, A.; Ruckenstuhl, C.; Dammbrueck, C.; Gross, A.S.; Herbst, V.; Carmona-Gutierrez, D.; Pietrocola, F.; Pieber, T.R.; Sigrist, S.J.; Linke, W.A.; Mühlfeld, C.; Sadoshima, J.; Dengjel, J.; Kiechl, S.; Kroemer, G.; Sedej, S.; Madeo, F. Dietary spermidine for lowering high blood pressure. *Autophagy*, **2017**, *13,* 767–769.

[114] Yuan, R.; Tsaih, S.-W.; Petkova, S.B.; Marin de Evsikova, C.; Xing, S.; Marion, M.A.; Bogue, M.A.; Mills, K.D.; Peters, L.L.; Bult, C.J.; Rosen, C.J.; Sundberg, J.P.; Harrison, D.E.; Churchill, G.A.; Paigen, B. Aging in inbred strains of mice: Study design and interim report on median lifespans and circulating IGF1 levels. *Aging cell*, **2009**, *8,* 277–287.

[115] Milman, S.; Atzmon, G.; Huffman, D.M.; Wan, J.; Crandall, J.P.; Cohen, P.; Barzilai, N. Low insulin-like growth factor-1 level predicts survival in humans with exceptional longevity. *Aging cell*, **2014**, *13,* 769–771.

[116] Inuzuka, Y.; Okuda, J.; Kawashima, T.; Kato, T.; Niizuma, S.; Tamaki, Y.; Iwanaga, Y.; Yoshida, Y.; Kosugi, R.; Watanabe-Maeda, K.; Machida, Y.; Tsuji, S.; Aburatani, H.; Izumi, T.; Kita, T.; Shioi, T. Suppression of phosphoinositide 3-kinase prevents cardiac aging in mice. *Circulation*, **2009**, *120,* 1695–1703.

[117] Laughlin, G.A.; Barrett-Connor, E.; Criqui, M.H.; Kritz-Silverstein, D. The prospective association of serum insulin-like growth factor I (IGF-I) and IGF-binding protein-1 levels with all cause and cardiovascular disease mortality in older adults: The Rancho Bernardo Study. *The Journal of clinical endocrinology and metabolism*, **2004**, *89,* 114–120.

[118] Rajeeve, V.; Pearce, W.; Cascante, M.; Vanhaesebroeck, B.; Cutillas, P.R. Polyamine production is downstream and upstream of oncogenic PI3K signalling and contributes to tumour cell growth. *The Biochemical journal*, **2013**, *450,* 619–628.

[119] Donohue, T.J.; Dworkin, L.D.; Lango, M.N.; Fliegner, K.; Lango, R.P.; Benstein, J.A.; Slater, W.R.; Catanese, V.M. Induction of myocardial insulin-like growth factor-I gene expression in left ventricular hypertrophy. *Circulation*, **1994**, *89,* 799–809.

[120] Pietrocola, F.; Lachkar, S.; Enot, D.P.; Niso-Santano, M.; Bravo-San Pedro, J.M.; Sica, V.; Izzo, V.; Maiuri, M.C.; Madeo, F.; Mariño, G.; Kroemer, G. Spermidine induces autophagy by inhibiting the acetyltransferase EP300. *Cell death and differentiation*, **2015**, *22,* 509–516.

[121] Stitt, T.N.; Drujan, D.; Clarke, B.A.; Panaro, F.; Timofeyva, Y.; Kline, W.O.; Gonzalez, M.; Yancopoulos, G.D.; Glass, D.J. The IGF-1/PI3K/Akt pathway prevents expression of muscle atrophy-induced ubiquitin ligases by inhibiting FOXO transcription factors. *Molecular cell*, **2004**, *14,* 395–403.

6   Appendix

Statistical tables – IGF-1R mice

IGF1-R

Pairwise Comparisons

Dependent Variable: IGF1R_log

Treatment	(I) Genotype	(J) Genotype	Mean Difference (I-J)	Std. Error	Sig.[b]	95% Confidence Interval for Difference[b]	
						Lower Bound	Upper Bound
CTRL	WT	IGF	-1.025*	.084	.000	-1.193	-.857
	IGF	WT	1.025*	.084	.000	.857	1.193
SPD	WT	IGF	-.626*	.086	.000	-.798	-.454
	IGF	WT	.626*	.086	.000	.454	.798

Based on estimated marginal means

*. The mean difference is significant at the .05 level.

b. Adjustment for multiple comparisons: Least Significant Difference (equivalent to no adjustments).

Pairwise Comparisons

Dependent Variable: IGF1R_log

Genotype	(I) Treatment	(J) Treatment	Mean Difference (I-J)	Std. Error	Sig.[b]	95% Confidence Interval for Difference[b]	
						Lower Bound	Upper Bound
WT	CTRL	SPD	-.162	.085	.060	-.331	.007
	SPD	CTRL	.162	.085	.060	-.007	.331
IGF	CTRL	SPD	.236*	.085	.007	.068	.405
	SPD	CTRL	-.236*	.085	.007	-.405	-.068

Based on estimated marginal means

*. The mean difference is significant at the .05 level.

b. Adjustment for multiple comparisons: Least Significant Difference (equivalent to no adjustments).

mTOR

Pairwise Comparisons

Dependent Variable: mtor_log

Treatment	(I) Genotype	(J) Genotype	Mean Difference (I-J)	Std. Error	Sig.[a]	95% Confidence Interval for Difference[a]	
						Lower Bound	Upper Bound
CTRL	WT	IGF	.009	.033	.785	-.057	.075
	IGF	WT	-.009	.033	.785	-.075	.057
SPD	WT	IGF	.018	.034	.594	-.050	.086
	IGF	WT	-.018	.034	.594	-.086	.050

Based on estimated marginal means

a. Adjustment for multiple comparisons: Least Significant Difference (equivalent to no adjustments).

Pairwise Comparisons

Dependent Variable: mtor_log

Genotype	(I) Treatment	(J) Treatment	Mean Difference (I-J)	Std. Error	Sig.[a]	95% Confidence Interval for Difference[a]	
						Lower Bound	Upper Bound
WT	CTRL	SPD	.021	.033	.534	-.046	.088
	SPD	CTRL	-.021	.033	.534	-.088	.046
IGF	CTRL	SPD	.030	.033	.372	-.037	.097
	SPD	CTRL	-.030	.033	.372	-.097	.037

Based on estimated marginal means

a. Adjustment for multiple comparisons: Least Significant Difference (equivalent to no adjustments).

Akt

Pairwise Comparisons

Dependent Variable: VAR00002

Treatment	(I) Genotype	(J) Genotype	Mean Difference (I-J)	Std. Error	Sig.[b]	95% Confidence Interval for Difference[b]	
						Lower Bound	Upper Bound
CTRL	WT	IGF	.289*	.040	.000	.209	.370
	IGF	WT	-.289*	.040	.000	-.370	-.209
SPD	WT	IGF	.275*	.042	.000	.191	.360
	IGF	WT	-.275*	.042	.000	-.360	-.191

Based on estimated marginal means

*. The mean difference is significant at the .05 level.

b. Adjustment for multiple comparisons: Least Significant Difference (equivalent to no adjustments).

Pairwise Comparisons

Dependent Variable: VAR00002

Genotype	(I) Treatment	(J) Treatment	Mean Difference (I-J)	Std. Error	Sig.[a]	95% Confidence Interval for Difference[a]	
						Lower Bound	Upper Bound
WT	CTRL	SPD	.046	.040	.258	-.035	.127
	SPD	CTRL	-.046	.040	.258	-.127	.035
IGF	CTRL	SPD	.032	.042	.445	-.051	.115
	SPD	CTRL	-.032	.042	.445	-.115	.051

Based on estimated marginal means

a. Adjustment for multiple comparisons: Least Significant Difference (equivalent to no adjustments).

p-Akt(Ser473)

Pairwise Comparisons

Dependent Variable: pAKTser473_LOG

Treatment	(I) Genotype	(J) Genotype	Mean Difference (I-J)	Std. Error	Sig.[b]	95% Confidence Interval for Difference[b]	
						Lower Bound	Upper Bound
CTRL	WT	IGF	-.583*	.098	.000	-.783	-.382
	IGF	WT	.583*	.098	.000	.382	.783
SPD	WT	IGF	-.783*	.101	.000	-.987	-.578
	IGF	WT	.783*	.101	.000	.578	.987

Based on estimated marginal means

*. The mean difference is significant at the .05 level.

b. Adjustment for multiple comparisons: Least Significant Difference (equivalent to no adjustments).

Pairwise Comparisons

Dependent Variable: pAKTser473_LOG

Genotype	(I) Treatment	(J) Treatment	Mean Difference (I-J)	Std. Error	Sig.[a]	95% Confidence Interval for Difference[a]	
						Lower Bound	Upper Bound
WT	CTRL	SPD	.199	.099	.052	-.002	.400
	SPD	CTRL	-.199	.099	.052	-.400	.002
IGF	CTRL	SPD	-.001	.099	.992	-.202	.200
	SPD	CTRL	.001	.099	.992	-.200	.202

Based on estimated marginal means

a. Adjustment for multiple comparisons: Least Significant Difference (equivalent to no adjustments).

p-Akt(Thr308)

Pairwise Comparisons

Dependent Variable: pAKTTr308_LOG

Treatment	(I) Genotype	(J) Genotype	Mean Difference (I-J)	Std. Error	Sig.[b]	95% Confidence Interval for Difference[b]	
						Lower Bound	Upper Bound
CTRL	WT	IGF	-.531*	.078	.000	-.689	-.372
	IGF	WT	.531*	.078	.000	.372	.689
SPD	WT	IGF	-.661*	.079	.000	-.822	-.499
	IGF	WT	.661*	.079	.000	.499	.822

Based on estimated marginal means

*. The mean difference is significant at the .05 level.

b. Adjustment for multiple comparisons: Least Significant Difference (equivalent to no adjustments).

Pairwise Comparisons

Dependent Variable: pAKTTr308_LOG

Genotype	(I) Treatment	(J) Treatment	Mean Difference (I-J)	Std. Error	Sig.[a]	95% Confidence Interval for Difference[a]	
						Lower Bound	Upper Bound
WT	CTRL	SPD	.059	.078	.454	-.100	.218
	SPD	CTRL	-.059	.078	.454	-.218	.100
IGF	CTRL	SPD	-.071	.078	.373	-.230	.088
	SPD	CTRL	.071	.078	.373	-.088	.230

Based on estimated marginal means

a. Adjustment for multiple comparisons: Least Significant Difference (equivalent to no adjustments).

Statistical tables – dnPI3K mice

mTOR

Pairwise Comparisons

Dependent Variable: mTOR_log

Treatment	(I) Genotype	(J) Genotype	Mean Difference (I-J)	Std. Error	Sig.[a]	95% Confidence Interval for Difference[a]	
						Lower Bound	Upper Bound
CTRL	WT	dnPI3K	-,050	,029	,095	-,108	,009
	dnPI3K	WT	,050	,029	,095	-,009	,108
SPD	WT	dnPI3K	-,020	,029	,488	-,079	,038
	dnPI3K	WT	,020	,029	,488	-,038	,079

Based on estimated marginal means

a. Adjustment for multiple comparisons: Least Significant Difference (equivalent to no adjustments).

Pairwise Comparisons

Dependent Variable: mTOR_log

Genotype	(I) Treatment	(J) Treatment	Mean Difference (I-J)	Std. Error	Sig.[a]	95% Confidence Interval for Difference[a]	
						Lower Bound	Upper Bound
WT	CTRL	SPD	,008	,029	,794	-,051	,066
	SPD	CTRL	-,008	,029	,794	-,066	,051
dnPI3K	CTRL	SPD	,037	,029	,214	-,022	,095
	SPD	CTRL	-,037	,029	,214	-,095	,022

Based on estimated marginal means

a. Adjustment for multiple comparisons: Least Significant Difference (equivalent to no adjustments).

Akt

Pairwise Comparisons

Dependent Variable: AKT_log

Treatment	(I) Genotype	(J) Genotype	Mean Difference (I-J)	Std. Error	Sig.[b]	95% Confidence Interval for Difference[b]	
						Lower Bound	Upper Bound
CTRL	WT	dnPI3K	-,229[*]	,031	,000	-,292	-,167
	dnPI3K	WT	,229[*]	,031	,000	,167	,292
SPD	WT	dnPI3K	-,150[*]	,031	,000	-,213	-,088
	dnPI3K	WT	,150[*]	,031	,000	,088	,213

Based on estimated marginal means

*. The mean difference is significant at the ,05 level.

b. Adjustment for multiple comparisons: Least Significant Difference (equivalent to no adjustments).

Pairwise Comparisons

Dependent Variable: AKT_log

Genotype	(I) Treatment	(J) Treatment	Mean Difference (I-J)	Std. Error	Sig.[a]	95% Confidence Interval for Difference[a]	
						Lower Bound	Upper Bound
WT	CTRL	SPD	-,056	,031	,077	-,118	,006
	SPD	CTRL	,056	,031	,077	-,006	,118
dnPI3K	CTRL	SPD	,023	,031	,465	-,039	,085
	SPD	CTRL	-,023	,031	,465	-,085	,039

Based on estimated marginal means

a. Adjustment for multiple comparisons: Least Significant Difference (equivalent to no adjustments).

p-Akt(Ser473)

Pairwise Comparisons

Dependent Variable: pAKT_ser_log

Treatment	(I) Genotype	(J) Genotype	Mean Difference (I-J)	Std. Error	Sig.[b]	95% Confidence Interval for Difference[b]	
						Lower Bound	Upper Bound
CTRL	WT	dnPI3K	,257[*]	,061	,000	,134	,380
	dnPI3K	WT	-,257[*]	,061	,000	-,380	-,134
SPD	WT	dnPI3K	,093	,061	,135	-,030	,216
	dnPI3K	WT	-,093	,061	,135	-,216	,030

Based on estimated marginal means

*. The mean difference is significant at the ,05 level.

b. Adjustment for multiple comparisons: Least Significant Difference (equivalent to no adjustments).

Pairwise Comparisons

Dependent Variable: pAKT_ser_log

Genotype	(I) Treatment	(J) Treatment	Mean Difference (I-J)	Std. Error	Sig.[b]	95% Confidence Interval for Difference[b]	
						Lower Bound	Upper Bound
WT	CTRL	SPD	-,008	,061	,900	-,131	,115
	SPD	CTRL	,008	,061	,900	-,115	,131
dnPI3K	CTRL	SPD	-,172*	,061	,007	-,295	-,049
	SPD	CTRL	,172*	,061	,007	,049	,295

Based on estimated marginal means

*. The mean difference is significant at the ,05 level.

b. Adjustment for multiple comparisons: Least Significant Difference (equivalent to no adjustments).

p-Akt(Thr308)

Pairwise Comparisons

Dependent Variable: pAKT_Thr_log

Treatment	(I) Genotype	(J) Genotype	Mean Difference (I-J)	Std. Error	Sig.[b]	95% Confidence Interval for Difference[b]	
						Lower Bound	Upper Bound
CTRL	WT	dnPI3K	,391*	,065	,000	,261	,522
	dnPI3K	WT	-,391*	,065	,000	-,522	-,261
SPD	WT	dnPI3K	,135*	,065	,042	,005	,266
	dnPI3K	WT	-,135*	,065	,042	-,266	-,005

Based on estimated marginal means

*. The mean difference is significant at the ,05 level.

b. Adjustment for multiple comparisons: Least Significant Difference (equivalent to no adjustments).

Pairwise Comparisons

Dependent Variable: pAKT_Thr_log

Genotype	(I) Treatment	(J) Treatment	Mean Difference (I-J)	Std. Error	Sig.[b]	95% Confidence Interval for Difference[b]	
						Lower Bound	Upper Bound
WT	CTRL	SPD	,153*	,065	,023	,023	,284
	SPD	CTRL	-,153*	,065	,023	-,284	-,023
dnPI3K	CTRL	SPD	-,103	,065	,120	-,233	,028
	SPD	CTRL	,103	,065	,120	-,028	,233

Based on estimated marginal means

*. The mean difference is significant at the ,05 level.

b. Adjustment for multiple comparisons: Least Significant Difference (equivalent to no adjustments).

p-FoxO3a

Pairwise Comparisons

Dependent Variable: pFOXO3_log

Treatment	(I) Genotype	(J) Genotype	Mean Difference (I-J)	Std. Error	Sig.[b]	95% Confidence Interval for Difference[b]	
						Lower Bound	Upper Bound
CTRL	WT	dnPI3K	,142	,083	,094	-,025	,309
	dnPI3K	WT	-,142	,083	,094	-,309	,025
SPD	WT	dnPI3K	-,151[*]	,064	,023	-,281	-,022
	dnPI3K	WT	,151[*]	,064	,023	,022	,281

Based on estimated marginal means

*. The mean difference is significant at the ,05 level.

b. Adjustment for multiple comparisons: Least Significant Difference (equivalent to no adjustments).

Pairwise Comparisons

Dependent Variable: pFOXO3_log

Genotype	(I) Treatment	(J) Treatment	Mean Difference (I-J)	Std. Error	Sig.[b]	95% Confidence Interval for Difference[b]	
						Lower Bound	Upper Bound
WT	CTRL	SPD	,282[*]	,064	,000	,152	,411
	SPD	CTRL	-,282[*]	,064	,000	-,411	-,152
dnPI3K	CTRL	SPD	-,012	,083	,889	-,179	,156
	SPD	CTRL	,012	,083	,889	-,156	,179

Based on estimated marginal means

*. The mean difference is significant at the ,05 level.

b. Adjustment for multiple comparisons: Least Significant Difference (equivalent to no adjustments).